

Possibility to measure thermal effects in the Casimir force

B. Geyer,¹ G. L. Klimchitskaya,^{1,2} and V. M. Mostepanenko^{1,3}

¹*Institute for Theoretical Physics, Leipzig University,*

Postfach 100920, D-04009, Leipzig, Germany

²*North-West Technical University, Millionnaya Street 5, St.Petersburg, 191065, Russia*

³*Noncommercial Partnership “Scientific Instruments”,*

Tverskaya Street 11, Moscow, 103905, Russia

Abstract

We analyze the possibility to measure small thermal effects in the Casimir force between metal test bodies in configurations of a sphere above a plate and two parallel plates. For sphere-plate geometry used in many experiments we investigate the applicability of the proximity force approximation (PFA) to calculate thermal effects in the Casimir force and its gradient. It is shown that for real metals the two formulations of the PFA used in the literature lead to relative differences in the obtained results being less than a small parameter equal to the ratio of separation distance to sphere radius. For ideal metals the PFA results for the thermal correction are obtained and compared with available exact results. It is emphasized that in the experimental region in the zeroth order of the small parameter mentioned above the thermal Casimir force and its gradient calculated using the PFA (and thermal corrections in their own right) coincide with respective exact results. For real metals available exact results are outside the application region of the PFA. However, the exact results are shown to converge to the PFA results when the small parameter goes down to the experimental values. We arrive at the conclusion that large thermal effects predicted by the Drude model approach, if existing at all, could be measured in both static and dynamic experiments in sphere-plate and plate-plate configurations. As to the small thermal effects predicted by the plasma model approach, the static experiment in the configuration of two parallel plates is found to be the best for its observation.

PACS numbers: 31.30.jh, 12.20.Ds, 12.20.Fv, 42.50.Nn

I. INTRODUCTION

The Casimir effect [1] is now universally known as one of the most extensively studied manifestations of zero-point oscillations. It attracts considerable attention in quantum field theory, gravitation and cosmology, atomic physics and optics, condensed matter physics, and in applications to nanotechnology (see monographs [2–6]). The fundamental theory describing both the van der Waals and Casimir forces between two semispaces with planar boundaries was developed by Lifshitz [7, 8]. At present the Lifshitz theory is generalized for material bodies with curved boundary surfaces (see, e.g., Refs. [9, 10]). Over a long period of years only a very limited experimental information about the Casimir force was available. Recently, however, a significant advance has been made in the experimental study of this phenomenon reflected in review [11]. In principle, the theoretical and experimental progress taken together allows computation and measurement of Casimir forces between bodies of complicated geometrical shape made of different materials. In order for such computation to be made, one should know the reflection amplitudes on the boundary surfaces at all Matsubara frequencies. At first sight this should present no problems because the reflection amplitudes can be either measured directly or calculated using measured material properties, such as frequency-dependent dielectric permittivities. At this point, however, difficulties emerge unexpectedly which are connected with the role of relaxation properties of charge carriers in the Casimir effect.

Beginning in 2000, the influence of relaxation on the thermal Casimir force was hotly debated. Boström and Sernelius [12] have noticed that the substitution of the dielectric permittivity of the Drude model with nonzero relaxation parameter into the Lifshitz formula results in a decreasing magnitude of the Casimir free energy and force as a function of temperature over a wide region of separations. This is in contradiction with the case of ideal metal plates or plate materials described by the nondissipative plasma model, where the magnitudes of the Casimir free energy and force are monotonously increasing functions of the temperature [13, 14]. At large separations (or in high temperature limit) the magnitudes of the Casimir free energy and force between metal plates calculated using the Drude model are by a factor of 2 less than the same quantities calculated for ideal metals or metals described by the plasma model. It was also shown that for metals with perfect crystal lattices the Lifshitz theory combined with the Drude model violates the Nernst heat theorem [6, 11, 15, 16]. For

metals with impurities leading to a nonzero relaxation at zero temperature Nernst's theorem was shown to be followed [17, 18]. This, however, does not solve the problem because perfect crystal metal is an idealized model of a truly equilibrium system with nondegenerate ground state for which the laws of thermodynamics must be satisfied.

A large thermal effect in the Casimir force between metals at separations of a few hundred nanometers predicted by the Lifshitz theory combined with the Drude model was experimentally excluded [19] by indirect dynamic measurements of the Casimir pressure in the configuration of a sphere above a plate of a micromachined oscillator. Later this experiment was repeated for two more times with increased precision. The exclusion of the thermal effect predicted by the Drude model was confirmed at a 95% confidence level [20, 21] and at a 99.9% confidence level [22, 23]. The same measurement data were found to be consistent with the Lifshitz theory combined with the plasma model. It is important to keep in mind that the comparison of experiment with theory in Refs. [19–23] was based on the use of an approximate method, the so-called *proximity force approximation* (PFA) [6, 11, 24] because at that time for sphere-plate configuration an exact theory was not available. At the moment there is a conceptual possibility to compute the thermal Casimir force between a sphere and a plate made of real metals with no use of the PFA [25, 26], but the region of experimental parameters is not yet achieved due to computational difficulties.

When it is considered that the Drude model correctly describes the relaxation of conduction electrons at low frequencies, the contradiction with basic laws of thermodynamics and disagreement with the experimental data outlined above are puzzling. These problems were dramatized by the demonstration that the inclusion of dc conductivity of dielectric (or dielectric-type semiconductor) materials into the model of dielectric response in the Lifshitz theory also results in a violation of the Nernst theorem [27–30]. From the experimental side, it was shown that the measurement data of the experiment on optical modulation of the Casimir force between Au sphere and Si plate with light [31, 32] excludes the Lifshitz theory taking into account the dc conductivity of dielectrics at a 95% confidence level. A similar result was obtained from the measurement of the Casimir-Polder force between the Bose-Einstein condensate of ^{87}Rb atoms and SiO_2 plate [33]. Here, the Lifshitz theory taking dc conductivity of SiO_2 into account was experimentally excluded at a 70% confidence level [34]. It is pertinent to note that while the comparison of the optical modulation experiment with theory uses the PFA, the measurement results for the Casimir-Polder force

were compared with the exact Lifshitz formula for atom-wall interaction. One can summarize that experiments with metals, semiconductors and dielectrics exclude the influence of dissipation of conduction electrons on the Casimir force (the statement on the opposite in the Introduction to Ref. [26] is a typo).

The conflict between such a fundamental theory, as the Lifshitz theory, thermodynamics and the experimental data of several experiments is a problem of great concern. Because of this, a lot of attempts to resolve this problem has been undertaken. Specifically, it was even suggested [35, 36] to modify the Lifshitz theory by including into consideration screening effects and diffusion currents. It was noted, however, that the modifications proposed do not alleviate contradictions with thermodynamics and the experimental data (discussion on this subject can be found in Refs. [37–42]). On the other hand, it was suggested [43] to modify the Planck distribution law by taking into account “saturation effects”. There were also attempts to soften contradictions with thermodynamics by reformulating the problem [44] and by finding additional statistical arguments in favor of the Drude model [45, 46]. In Ref. [47], in addition to the usually used exponential screening, the so-called *algebraic screening* in atom-wall interaction was considered. As a result, linear in temperature thermal correction to the Casimir-Polder force at short separations was predicted similar to that predicted by the Drude model. Note that the algebraic screening is connected with nonanalytic terms in the small wavenumber expansion of the dielectric permittivity. It was finally suggested [48] that for the resolution of the problem some concepts of statistical physics related to the theoretical description of the interaction of classical and quantum fluctuating fields with matter might need a reconsideration.

The prospects for a pure theoretical resolution of the above problems seem dim at the moment. In this situation any additional experimental evidence could be very useful. In this paper we analyze the possibility to measure thermal effects in the Casimir force on the basis of already created and used experimental setups. We stress that in the experiments [19–23, 31, 32] mentioned above the large thermal correction to the Casimir force, as predicted by the Drude model, was excluded. However, these experiments were not of sufficient precision to measure the thermal effect for metals predicted by the plasma model or for dielectrics with dc conductivity omitted (till the moment the thermal effect was measured in the Casimir-Polder force alone [33]). Keeping in mind that there is some confusion in the literature concerning the use of the PFA, we present two (not equivalent) formulations of the PFA and

clarify which of them was really used in the comparison between experiment and theory. We especially analyze the calculation results for the thermal correction to the Casimir force in sphere-plate configuration found using the PFA and explain when they are meaningful. The obtained conclusions are confirmed by the comparison with exact results for the thermal contribution to the Casimir force between a sphere and a plate. We show that at the moment it is not possible to measure small thermal effects in the Casimir force (or its gradient) in sphere-plate geometry, as predicted by the Lifshitz formula combined with the plasma model. We also discuss the configuration of two parallel plates in both dynamic and static regimes. According to our results, small thermal corrections to the gradient of the Casimir pressure in the dynamic regime is suppressed. The only way to measure small thermal effects in the Casimir pressure is suggested by the configuration of two parallel plates in the static regime.

The paper is organized as follows. In Sec. II two different formulations of the PFA are considered and applied to the Casimir force in sphere-plate configuration. Section III discusses the same subject with respect to the gradient of the Casimir force between a sphere and a plate. In Sec. IV the relationship between the PFA and the exact results is presented for a sphere and a plate made of ideal metal. The applicability of the PFA to describe thermal corrections to the Casimir force between a sphere and a plate made of real metals and the possibility to measure the thermal effect are considered in Sec. V. In Sec. VI we show that the static Casimir configuration of two parallel plates is preferential for the observation of a small thermal effect in the Casimir pressure. Section VII contains our conclusions and discussion.

II. THE PROXIMITY FORCE APPROXIMATION FOR THE CASIMIR FORCE BETWEEN A SPHERE AND A PLATE

Different authors vary somewhat in the meaning of the term “PFA”. In fact the term “proximity force theorem” (later changed for PFA) was introduced in Ref. [24] where the so-called *Derjaguin method* [49] was applied in order to calculate the force acting between curved surfaces by using the known force per unit area of plane parallel plates. In the Derjaguin method, the unknown force between the elements of curved surfaces is approximately replaced with a known force per unit area of plane surfaces at respective separations. In application to a sphere of radius R above a plane surface of a plate $z = 0$ the Derjaguin

method represents the force between them in the form

$$F_{\text{sp}}(a, T) = \int_{\Sigma} d\sigma P(z, T). \quad (1)$$

Here, $d\sigma$ is the element of plate area, Σ is the projection of the sphere onto the plate, a is the shortest separation between the sphere and the plate, and $P(z, T)$ is the force per unit area of two plane parallel plates at a separation z at temperature T (i.e., the Casimir pressure). Choosing the origin of a cylindrical coordinate system on the plane $z = 0$ under the sphere center, the coordinate z of any point on the sphere is given by $z = R + a - (R^2 - \rho^2)^{1/2}$. Then Eq. (1) leads to

$$\begin{aligned} F_{\text{sp}}(a, T) &= 2\pi \int_0^R \rho d\rho P(z, T) \\ &= 2\pi \int_a^{R+a} (R + a - z) P(z, T) dz. \end{aligned} \quad (2)$$

Keeping in mind that the thermal Casimir pressure is connected with the free energy per unit area of two parallel plates as

$$P(z, T) = -\frac{\partial \mathcal{F}_{\text{pp}}(z, T)}{\partial z}, \quad (3)$$

and integrating by parts in Eq. (2), one arrives at

$$F_{\text{sp}}(a, T) = 2\pi R \mathcal{F}_{\text{pp}}(a, T) - 2\pi \int_a^{R+a} dz \mathcal{F}_{\text{pp}}(z, T). \quad (4)$$

This generalizes Eq. (20) of Ref. [50] related to the nonretarded case.

Further simplification of Eq. (4) can be achieved when it is assumed that the free energy $\mathcal{F}_{\text{pp}}(z, T)$ is a quickly decreasing function of z and drops to zero on the characteristic length of about the sphere radius R . Let us consider the case of the free energy of the Casimir interaction given by the Lifshitz formula,

$$\mathcal{F}_{\text{pp}}(z, T) = \frac{k_B T}{2\pi} \sum_{l=0}^{\infty}{}' \int_0^{\infty} k_{\perp} dk_{\perp} \sum_{\alpha} \ln(1 - r_{\alpha}^2 e^{-2q_l z}). \quad (5)$$

Here, k_B is the Boltzmann constant, the prime near the summation sign multiplies the term with $l = 0$ by $1/2$, k_{\perp} is the projection of the wave vector on the plane of plates, and $q_l = (k_{\perp}^2 + \xi_l^2/c^2)^{1/2}$ where $\xi_l = 2\pi k_B T l / \hbar$ with $l = 0, 1, 2, \dots$ are the Matsubara frequencies. The reflection coefficients r_{α} for the two polarizations of the electromagnetic

field, transverse magnetic ($\alpha = \text{TM}$) and transverse electric ($\alpha = \text{TE}$), are expressed in terms of the dielectric permittivity along the imaginary frequencies,

$$\begin{aligned} r_{\text{TM}} &= r_{\text{TM}}(i\xi_l, k_{\perp}) = \frac{\varepsilon(i\xi_l)q_l - k_l}{\varepsilon(i\xi_l)q_l + k_l}, \\ r_{\text{TE}} &= r_{\text{TE}}(i\xi_l, k_{\perp}) = \frac{q_l - k_l}{q_l + k_l}, \\ k_l &= \left[k_{\perp}^2 + \varepsilon(i\xi_l) \frac{\xi_l^2}{c^2} \right]^{1/2}. \end{aligned} \quad (6)$$

In order to simplify Eq. (4), we use an expansion in power series in Eq. (5):

$$\mathcal{F}_{\text{pp}}(z, T) = -\frac{k_B T}{2\pi} \sum_{l=0}^{\infty} \sum_{n=1}^{\infty} \frac{1}{n} \int_0^{\infty} k_{\perp} dk_{\perp} \sum_{\alpha} r_{\alpha}^{2n} e^{-2q_l n z}. \quad (7)$$

Then from Eq. (7) one finds

$$\begin{aligned} I(a, T) &\equiv - \int_a^{R+a} dz \mathcal{F}_{\text{pp}}(z, T) = \frac{k_B T}{4\pi} \sum_{l=0}^{\infty} \sum_{n=1}^{\infty} \frac{1}{n^2} \\ &\times \int_0^{\infty} \frac{k_{\perp} dk_{\perp}}{q_l} \sum_{\alpha} r_{\alpha}^{2n} [e^{-2q_l n a} - e^{-2q_l n (R+a)}]. \end{aligned} \quad (8)$$

When R goes to infinity with a and T fixed, the contribution to $I(a, T)$ of the second term in square brackets on the right-hand side of Eq. (8) vanishes as $(R+a)^{-1}$. This means that for large R the value of $I(a, T)$ is determined by the first term in square brackets and can be considered as independent on R . Hence, rewriting Eq. (4) in the form

$$F_{\text{sp}}(a, T) = 2\pi R \mathcal{F}_{\text{pp}}(a, T) \left[1 + \frac{I(a, T)}{R \mathcal{F}_{\text{pp}}(a, T)} \right], \quad (9)$$

one concludes that in the limit of large R it holds $I(a, T)/R \mathcal{F}_{\text{pp}}(a, T) \sim C/R$ where C is some constant.

Let us now consider the behavior of the quantity $I/R \mathcal{F}_{\text{pp}}$ in the limiting case $a \rightarrow 0$ keeping R fixed. This is a nonrelativistic limit where [6, 51]

$$\mathcal{F}_{\text{pp}}(a, T) = E_{\text{pp}}(a) = -\frac{H}{12\pi a^2}, \quad I(a, T) = \frac{RH}{12\pi a(R+a)} \quad (10)$$

with the Hamaker constant defined by

$$H = \frac{3\hbar}{8\pi} \int_0^{\infty} d\xi \int_0^{\infty} y^2 dy \left\{ \left[\frac{\varepsilon(i\xi) + 1}{\varepsilon(i\xi) - 1} \right]^2 e^y - 1 \right\}^{-1}. \quad (11)$$

From Eq. (10) it follows $I(a, T)/R\mathcal{F}_{\text{pp}}(a, T) \sim Ca$ when a vanishes. Thus Eq. (9) can be rewritten as

$$F_{\text{sp}}(a, T) = 2\pi R\mathcal{F}_{\text{pp}}(a, T) \left[1 + f(a, T) \frac{a}{R} \right], \quad (12)$$

where $f(a, T)$ is scarcely affected by the sphere radius R . For all models of dielectric permittivity used to describe metals the magnitude of $f(a, T)$ is less than unity over wide ranges of experimental parameters (see below the results of numerical computations).

Under the condition $a \ll R$ which is usually valid in experiments on measuring the Casimir force one may neglect the term of order a/R on the right-hand side of Eq. (12) and arrives at

$$F_{\text{sp}}(a, T) = 2\pi R\mathcal{F}_{\text{pp}}(a, T). \quad (13)$$

Just this equation was called the ‘‘proximity force theorem’’ in Ref. [24] and heavily used in the comparison of experiment with theory in all measurements of the Casimir force in sphere-plate geometry (see, e.g., Refs. [31, 32, 52–62]). As can be seen from the above derivation, Eq. (13) follows from Eq. (1) under some conditions, but is not equivalent to it. Because of this, to avoid confusion, Ref. [63] suggested to call (1) the *most general formulation* of the PFA and (13) the *simplified formulation* of the PFA. Keeping in mind that the used in experiments simplified formulation is obtained by disregarding contributions of order a/R , it would be meaningless to attribute physical meaning to any terms of order a/R in the thermal Casimir force F_{sp} calculated by using Eq. (13) (see discussion in Secs. IV and V).

One further version of the PFA discussed in the literature [64, 65] is connected with the choice of parallel surface elements in Eq. (1). In the original Derjaguin method [49] used by us the surface elements representing the sphere are parallel to the surface of the plate $z = 0$. In this case Σ is a part of the plane $z = 0$ (the so-called *plate-based* PFA). If, however, the lower half of the sphere is chosen as Σ [64], the plane elements representing the sphere are tangential to it and respective twin elements of the plate are tilted by different angles with respect to the plane $z = 0$ (the so-called *sphere-based* PFA). In both cases, the distance between the elements is measured along the normal to Σ . It was shown [64] that both the plate-based and sphere-based PFA lead to coinciding results in the zeroth order of a/R , i.e., to Eq. (13). The form of the function $f(a, T)$ in Eq. (12) for both versions of the PFA is, however, different. Basing on this, Refs. [65, 66] considered the results for the Casimir energies and forces obtained by PFA as ambiguous. The differences between the two

versions of the PFA were treated as some “error bars” inherent to this approximate method. Keeping in mind, however, that the comparison of experiment with theory in sphere-plate geometry is based not on the general formulation of the PFA (1), but on an unambiguous simplified formulation (13), the discussion of inherent to PFA errors is immaterial. In fact, when speaking about the Casimir force, only the zeroth order in a/R results in any of the PFA formulations are of physical significance and only under the condition $a \ll R$.

The situation changes drastically when, instead to the Casimir force, the PFA is applied, for instance, to the gravitational force. According to Refs. [63, 67], the most general formulation of the PFA (1) leads to an exact result for the force between a sphere and a plate for all conservative volumetric forces, particularly for the gravitational force. In so doing, however, only the original Derjaguin choice of Σ (plate-based) must be used. This makes the plate-based version of the PFA preferable in comparison with the sphere-based version.

Now we present the results of numerical computations for the function $f(a, T)$ defined in Eq. (12) in typical regions of experimental parameters. Computations were performed by using the Lifshitz formula (5) and Eq. (8) for a sphere and a plate made of Au. The dielectric properties of Au were described by using three different models. As a crude approximation, the model of ideal metal bodies was used leading to $r_{\text{TM}}(i\xi_l, k_\perp) = 1$, $r_{\text{TE}}(i\xi_l, k_\perp) = -1$. A frequently used description obtains the dielectric permittivity $\varepsilon(i\xi_l)$ by means of the Kramers-Kronig relation

$$\varepsilon(i\xi_l) = 1 + \frac{2}{\pi} \int_0^\infty \frac{\omega \text{Im} \varepsilon(\omega)}{\omega^2 + \xi_l^2} d\omega, \quad (14)$$

where $\text{Im} \varepsilon(\omega)$ is taken from tables of the optical data for Au [68] extrapolated to low frequencies by means of the Drude model

$$\text{Im} \varepsilon(\omega) = \frac{\omega_p^2 \gamma}{\omega(\omega^2 + \gamma^2)}. \quad (15)$$

Here, the plasma frequency and the relaxation parameter of Au are given by $\omega_p = 9.0$ eV, $\gamma = 0.035$ eV [69]. As one more alternative description used in the literature we have applied the generalized plasma-like model [6, 11, 23]

$$\varepsilon(i\xi_l) = 1 + \frac{\omega_p^2}{\xi_l^2} + \sum_{j=1}^6 \frac{g_j}{\omega_j^2 + \xi_l^2 + \gamma_j \xi_l}, \quad (16)$$

where $\omega_j \neq 0$ are the resonant frequencies of the oscillators describing core electrons, γ_j are the relaxation frequencies, and g_j are the oscillator strengths. The values of all these

parameters for Au can be found in [6, 23]. Note that there are proposals in the literature for alternative dielectric functions taking into account the effect of spatial nonlocality (see, for instance, Refs. [42, 70, 71]). However, for metallic test bodies these dielectric functions predict precisely the same thermal effect as the Drude model approach [41, 70, 71]. Because of this, they do not require a special consideration here.

In Fig. 1 the computational results for $f(a, T)$ are shown as a function of (a) separation at room temperature $T = 300$ K and (b) temperature at a separation $a = 2 \mu\text{m}$. In both cases a sphere with $R = 100 \mu\text{m}$ radius is used. The dotted, dashed and solid lines demonstrate the results obtained using ideal metals, Au described by the optical data extrapolated by the Drude model and Au described by the generalized plasma-like model, respectively. As can be seen in Fig. 1(a), in the region of separations from 100 nm to $5 \mu\text{m}$ it holds $0.5 \leq |f(a, T)| < 1$. It can be easily verified that in the limiting case $a \rightarrow 0$ the function $f(a, T) \rightarrow -1/2$ for ideal metals (the dotted line) and $f(a, T) \rightarrow -1$ for real Au independently of the model used for its description (the dashed and solid lines). From Fig. 1(b) it is seen that at any temperature from absolute zero to 300 K the magnitudes of $f(a, T)$ remain less than unity and the difference between various models of dielectric properties disappears with vanishing temperature.

Now we consider the measure of dependence of the function $f(a, T)$ on the sphere radius. The computational results for $f(a, T)$ as a function of $\log_{10}(a/R)$ are shown in Fig. 2 as the three groups of lines (dotted, dashed and solid for ideal metals and real Au described using the Drude and plasma models as explained above) numerated 1, 2, and 3 for fixed separations $a = 0.1, 2,$ and $5 \mu\text{m}$, respectively. Computations are done at room temperature $T = 300$ K for a/R varying from 10^{-4} to 0.05 . For example, as is seen in Fig. 2, at $a = 0.1 \mu\text{m}$ (the group 1 of lines) there is almost no dependence of $f(a, T)$ on R for radii larger than $2 \mu\text{m}$. For $a = 2 \mu\text{m}$ (the group 2 of lines) $f(a, T)$ does not depend on R for radii $R > 200 \mu\text{m}$. We remind that typical sphere radii are $R = 100 \mu\text{m}$ in the experiments [31, 32, 53–62] and $R = 150 \mu\text{m}$ in the experiments [20–23], performed at separations from less than 100 nm to a few hundred nanometers. In Fig. 2 it is seen also that the relative magnitude of the function $f(a, T)$ computed using different models of dielectric permittivity of Au depends on separation. For example, at $a = 0.1 \mu\text{m}$ $|f(a, T)|$ computed using the model of ideal metals (the dotted line) is less than using the generalized plasma-like model (the solid line) and using the tabulated optical data extrapolated by the Drude model (the dashed line).

At separations $a = 2$ and $5 \mu\text{m}$ the magnitude of $f(a, T)$ computed using the model of ideal metals is sandwiched between lines computed using the two models of real Au.

The size of possible corrections to the simplified formulation of the PFA (13) has been investigated experimentally by measuring the Casimir force between an Au-coated plate and five Au-coated spheres with different radii using a micromachined oscillator [72]. In so doing spheres with radii $R = 10.5, 31.4, 52.3, 102.8$ and $148.2 \mu\text{m}$ were used. The obtained constraint $|f(a, T)| \leq 0.6$ for $a < 300 \text{ nm}$, $T = 300 \text{ K}$ is in very good agreement with the computational results in Fig. 1(a). Thus, the experimental data are in favor of the simplified formulation of the PFA.

III. THE PROXIMITY FORCE APPROXIMATION FOR THE GRADIENT OF THE CASIMIR FORCE BETWEEN A SPHERE AND A PLATE

In many experiments using the sphere-plate configuration separation distance between the test bodies was varied harmonically (see, e.g., Refs. [6, 11, 19–23]). In this case not the Casimir force but its gradient is the physical quantity immediately connected with the frequency shift of a micromachined oscillator. The gradient of the Casimir force acting between a sphere and a plate can be found by differentiating Eq. (4) with respect to a and taking into account Eq. (3),

$$\frac{\partial F_{\text{sp}}(a, T)}{\partial a} = -2\pi RP(a, T) + 2\pi \mathcal{F}_{\text{pp}}(a, T) - 2\pi \mathcal{F}_{\text{pp}}(R + a, T). \quad (17)$$

Using Eq. (7) this can be rearranged to the form

$$\frac{\partial F_{\text{sp}}(a, T)}{\partial a} = -2\pi RP(a, T) \left[1 + \frac{J(a, T)}{RP(a, T)} \right], \quad (18)$$

where the following notation is introduced:

$$J(a, T) \equiv \frac{k_B T}{2\pi} \sum_{l=0}^{\infty} \sum_{n=1}^{\infty} \frac{1}{n} \int_0^{\infty} k_{\perp} dk_{\perp} \sum_{\alpha} r_{\alpha}^{2n} \times [e^{-2q_l n a} - e^{-2q_l n (R+a)}]. \quad (19)$$

Similar to Sec. II, it can easily be shown that at large R , with a and T fixed, it holds $J(a, T)/RP(a, T) \sim C/R$. On the other hand, in the nonrelativistic limit

$$P(a, T) = -\frac{H}{6\pi a^3}, \quad J(a, T) = \frac{RH(R + 2a)}{12\pi a^2 (R + a)^2}, \quad (20)$$

where H is defined in Eq. (11). From this it follows that $J(a, T)/RP(a, T) \sim Ca$ when a vanishes and R is kept constant. Thus, Eq. (18) can be rewritten in an equivalent form

$$\frac{\partial F_{\text{sp}}(a, T)}{\partial a} = -2\pi RP(a, T) \left[1 + p(a, T) \frac{a}{R} \right], \quad (21)$$

where $p(a, T)$ is scarcely affected by R . Below we demonstrate that in wide ranges of experimental parameters $p(a, T)$ is a very slowly varying function and $|p(a, T)| < 1/2$. Because of this, under the experimental condition $a \ll R$ we can neglect the term of order a/R in Eq. (21) and arrive at the equality

$$\frac{\partial F_{\text{sp}}(a, T)}{\partial a} = -2\pi RP(a, T), \quad (22)$$

which is the simplified formulation of the PFA for a gradient of the Casimir force in sphere-plate configuration. Equation (22) was used for the comparison of experiment with theory in dynamic measurements of the Casimir pressure [19–23, 73].

We have performed numerical computations of the quantity $p(a, T)$ as a function of separation and temperature for a sphere of fixed radius $R = 100 \mu\text{m}$. In Fig. 3(a) the computational results for $p(a, T)$ as a function of a are presented at $T = 300 \text{ K}$. Figure 3(b) shows $p(a, T)$ as a function of T at $a = 2 \mu\text{m}$. In both cases dotted, dashed and solid lines indicate the use of ideal metal surfaces and Au surfaces described by the Drude and plasma model approaches. As can be seen in Fig. 3(a), within the separation region from 100 nm to $5 \mu\text{m}$ the function $|p(a, T)|$ varies between 0.31 and 0.48. When the temperature increases from absolute zero to $T = 300 \text{ K}$, $|p(a, T)|$ remains sandwiched between 0.31 and 0.39 [see Fig. 3(b)]. This demonstrates that possible corrections to the simplified formulation of the PFA (22) do not exceed a/R .

It can be easily seen that the magnitude of $p(a, T)$ almost does not depend on the radius of the sphere. In Fig. 4 we present the computational results for $p(a, T)$ as a function of $\log_{10}(a/R)$ at $T = 300 \text{ K}$. The groups of lines numbered 1 and 2 are for the separations $a = 0.1$ and $5 \mu\text{m}$, respectively. The dotted, dashed and solid lines have the same meaning as in Figs. 1–3. As is seen in Fig. 4, for the group of lines 1 there is no dependence on a/R over the whole range from 10^{-4} to 0.05. Thus, at $a = 0.1 \mu\text{m}$, $p(a, T)$ does not depend on R for $R \geq 2 \mu\text{m}$. For the group of lines 2, $p(a, T)$ does not depend on R for $10^{-4} \leq a/R \leq 10^{-3}$. At $a = 5 \mu\text{m}$ this leads to $R \geq 5000 \mu\text{m}$. From Fig. 4 it also follows that relative magnitudes of the function $p(a, T)$ computed using different models of dielectric properties of metal depend on separation.

The experimental constraint on the magnitude of the correction to Eq. (22) was obtained in Ref. [72] by using several spheres with different radii (see Sec. II). In the separation region $a < 300$ nm at $T = 300$ K it was shown that $|p(a, T)| < 0.4$ at a 95% confidence level. This is in very good agreement with the computational results in Fig. 4 and provides the experimental confirmation for the simplified formulation of the PFA in application to the gradient of the thermal Casimir force between a sphere and a plate.

IV. RELATIONSHIP BETWEEN THE PROXIMITY FORCE APPROXIMATION AND EXACT RESULTS FOR IDEAL METALS

In what follows we apply the PFA to calculate the thermal Casimir force between a sphere and a plate made of ideal metal and discuss the possibility to describe the thermal correction using this approximate method. Using the notation (8), Eq. (4) for the thermal Casimir force can be presented in the form

$$\begin{aligned} F_{\text{sp}}(a, T) &= 2\pi R\mathcal{F}_{\text{pp}}(a, T) + 2\pi I(a, T) \\ &\equiv 2\pi R\mathcal{F}_{\text{pp}}(a, T) + 2\pi X(a, T) - 2\pi X(R + a, T). \end{aligned} \quad (23)$$

For ideal metals, using the dimensionless variables

$$y = 2aq_l, \quad \frac{2a\xi_l}{c} \equiv \tau_a l \quad (24)$$

in Eq. (8), the quantity $X(a, T)$ is given by

$$\begin{aligned} X(a, T) &= \frac{k_B T}{4\pi a} \sum'_{l=0}^{\infty} \sum_{n=1}^{\infty} \frac{1}{n^2} \int_{\tau_a l}^{\infty} dy e^{-ny} \\ &= \frac{k_B T}{8\pi a} \sum_{l=-\infty}^{\infty} \int_{\tau_a |l|}^{\infty} dy \text{Li}_2(e^{-y}), \end{aligned} \quad (25)$$

where $\text{Li}_n(z)$ is a polylogarithm function.

Equation (25) can be presented in an equivalent form convenient for the transition to the low-temperature limit using the Poisson summation formula [5, 6]. According to this formula, if $c(\alpha)$ is the Fourier transform of a function $b(x)$, i.e.

$$c(\alpha) = \frac{1}{2\pi} \int_{-\infty}^{\infty} b(x) e^{-i\alpha x} dx, \quad (26)$$

then it follows that

$$\sum_{l=-\infty}^{\infty} b(l) = 2\pi \sum_{l=-\infty}^{\infty} c(2\pi l). \quad (27)$$

Now we return to Eq. (25) and put

$$b(l) = \frac{k_B T}{8\pi a} \int_{\tau_a |l|}^{\infty} dy \text{Li}_2(e^{-y}). \quad (28)$$

Keeping in mind that $b(l) = b(-l)$ and using Eq. (26), one obtains

$$\begin{aligned} c(2\pi l) &= \frac{1}{\pi} \int_0^{\infty} b(x) \cos(2\pi l x) dx \\ &= \frac{\hbar c}{32\pi^3 a^2} \int_0^{\infty} dv \cos(l t_a v) \int_v^{\infty} dy \text{Li}_2(e^{-y}). \end{aligned} \quad (29)$$

Here, we have introduced a new variable $v = \tau_a x$ and the notation $t_a \equiv T_a/T$, where $k_B T_a \equiv \hbar c/(2a)$ is the effective temperature related to the separation distance between the sphere and the plate. Note that in terms of this notation it holds $\tau_a = 2\pi/t_a = 2\pi T/T_a$. Taking into account that the quantity $c(2\pi l)$ is an even function of its argument and using Eqs. (27) and (29), we arrive at

$$\begin{aligned} X(a, T) &= 4\pi \sum_{l=0}^{\infty}{}' c(2\pi l) \\ &= \frac{\hbar c}{8\pi^2 a^2} \sum_{l=0}^{\infty}{}' \int_0^{\infty} dy \text{Li}_2(e^{-y}) \int_0^y dv \cos(l t_a v), \end{aligned} \quad (30)$$

where we exchanged the order of integrations with respect to v and to y .

Equation (30) can be represented in the form

$$X(a, T) = \frac{\hbar c}{8\pi^2 a^2} \left[\frac{1}{2} X_0 + \sum_{l=1}^{\infty} X_l \right], \quad (31)$$

where

$$\begin{aligned} X_0 &= \int_0^{\infty} y dy \text{Li}_2(e^{-y}), \\ X_l &= \frac{1}{l t_a} \int_0^{\infty} dy \text{Li}_2(e^{-y}) \sin(l t_a y). \end{aligned} \quad (32)$$

Direct calculation leads to

$$\begin{aligned} X_0 &= \sum_{n=1}^{\infty} \frac{1}{n^4} \int_0^{\infty} x dx e^{-x} = \frac{\pi^4}{90}, \\ X_l &= \frac{1}{l t_a} \sum_{n=1}^{\infty} \frac{1}{n^3} \int_0^{\infty} dx e^{-x} \sin \frac{l t_a x}{n} \\ &= \sum_{n=1}^{\infty} \frac{1}{n^2(n^2 + l^2 t_a^2)} = \frac{1}{2l^4 t_a^4} + \frac{\pi^2}{6l^2 t_a^2} - \frac{\pi}{2} \frac{\coth(\pi l t_a)}{l^3 t_a^3}, \end{aligned} \quad (33)$$

where $x = ny$. Substituting Eq. (33) into Eq. (31), we obtain

$$X(a, T) = \frac{\pi^2 \hbar c}{1440a^2} \left[1 + \frac{5}{t_a^2} - \frac{90}{\pi^3 t_a^3} \sum_{l=1}^{\infty} \frac{\coth(\pi l t_a)}{l^3} + \frac{1}{t_a^4} \right]. \quad (34)$$

In the low-temperature limit it holds $T \ll T_a$, $t_a \gg 1$ and Eq. (34) results in

$$X(a, T) = \frac{\pi^2 \hbar c}{1440a^2} \left[1 + 5 \left(\frac{T}{T_a} \right)^2 - \frac{90\zeta(3)}{\pi^3} \left(\frac{T}{T_a} \right)^3 + \left(\frac{T}{T_a} \right)^4 \right], \quad (35)$$

where $\zeta(z)$ is the Riemann zeta function.

The quantity $X(R+a, T)$ in Eq. (23) is given by Eq. (34) where a is replaced with $R+a$, t_a is replaced with $t_R = T_R/T$ and T_R is defined from

$$k_B T_R = \frac{\hbar c}{2(R+a)} \approx \frac{\hbar c}{2R}. \quad (36)$$

The sphere radius introduces a second characteristic temperature into the problem which is much less than T_a in experimentally relevant situations. As an example, for typical spheres used in experiments on measuring the Casimir force $R = 100 \mu\text{m}$ and $a = 100 \text{nm}$ resulting in $T_R = 11.4 \text{K}$ and $T_a = 11400 \text{K}$. Thus, for experiments performed at room temperature, $T = 300 \text{K}$, it holds $T \ll T_a$, but $T \gg T_R$, i.e., a high-temperature regime with respect to the sphere radius, but a low-temperature regime with respect to the separation between the sphere and the plate.

Nevertheless, we begin with the case of extremely low temperature with respect to both parameters, $T \ll T_R \ll T_a$, which is achieved only well below 1 K. In this case the quantity $X(R+a, T)$ is also given by Eq. (35) where a is replaced with $R+a$ and T_a is replaced with T_R . We also take into account that under the condition $T \ll T_a$ the free energy between two plane parallel plates in Eq. (23) is given by [5, 6]

$$\mathcal{F}_{\text{pp}}(a, T) = -\frac{\pi^2 \hbar c}{720a^3} \left[1 + \frac{45\zeta(3)}{\pi^3} \left(\frac{T}{T_a} \right)^3 - \left(\frac{T}{T_a} \right)^4 \right]. \quad (37)$$

Substituting Eq. (37) and Eq. (35) (with the characteristic temperatures T_a and T_R) into Eq. (23), we arrive at the result

$$F_{\text{sp}}(a, T) = -\frac{\pi^3 \hbar c R}{360a^3} \left[1 - \frac{a}{2R} + \frac{a^3}{2R^3} \left(\frac{T}{T_R} \right)^4 \right]. \quad (38)$$

Here, we have included the main T -independent term of order a/R and the first nonvanishing term depending on temperature. The latter is of order T^4 and is multiplied by the third power of the small parameter a/R . For typical experimental parameters mentioned above $a/R \sim 10^{-3}$. If one puts $T = 1$ K [the highest temperature where Eq. (38) is applicable] the T -dependent term on the right-hand side of Eq. (38) appears to be of order 10^{-13} .

Equation (38) can be identically rewritten in the form

$$F_{\text{sp}}(a, T) = -\frac{\pi^3 \hbar c R}{360 a^3} \left(1 - \frac{a}{2R}\right) + \Delta_T F_{\text{sp}}(a, T), \quad (39)$$

where the thermal correction to the Casimir force is given by

$$\Delta_T F_{\text{sp}}(a, T) = -\frac{\pi^3 R^2 (k_B T)^4}{45 (\hbar c)^3}. \quad (40)$$

It is interesting to compare this result obtained using the general formulation of the PFA with the exact result for the thermal correction in sphere-plate configuration [74]. In the functional determinant representation the exact free energy of the Casimir interaction in sphere-plane geometry can be written as

$$\mathcal{F}_{\text{sp}}^{\text{exact}}(a, T) = \frac{k_B T}{2} \sum_{l=-\infty}^{\infty} \text{Tr} \ln [1 - M(a, \xi_l)], \quad (41)$$

where the explicit form of the matrix M in ideal metal case is contained in Ref. [74]. In the limit of extremely low temperature, $T \ll T_R$, and small separation distances, $a \ll R$, Ref. [74] arrives at the following exact result for the temperature-dependent part of the free energy

$$\Delta_T \mathcal{F}_{\text{sp}}^{\text{exact}}(a, T) = \frac{\pi^3 R^3 (k_B T)^4}{225 (\hbar c)^3} \left(\frac{29}{3} + \frac{112}{5} \frac{a}{R} \right). \quad (42)$$

From this equation, the exact thermal correction to the Casimir force in the limiting case under consideration is the following

$$\Delta_T F_{\text{sp}}^{\text{exact}}(a, T) = -\frac{\partial \Delta_T \mathcal{F}_{\text{sp}}^{\text{exact}}(a, T)}{\partial a} = -\frac{112 \pi^3 R^2 (k_B T)^4}{1125 (\hbar c)^3}. \quad (43)$$

It can be seen from the comparison of Eqs. (40) and (43) that although the most general formulation of the PFA gives the correct dependence of the thermal correction on the fourth power of T , the numerical coefficient before it is underestimated by a factor of 4.48. At the same time, the application of the simplified formulation of the PFA (13) in this limiting case results in an incorrect dependence of the thermal correction on T (the third power of

T instead of the fourth). These results are not surprising. As explained in Sec. II, the PFA is applicable only under the condition $a \ll R$ and leads to reliable predictions which are of zeroth order in the small parameter a/R . Because of this, any contribution either to the free energy or to the force which relative magnitude is numerically of about a/R or smaller calculated using the PFA must be disregarded as physically meaningless. Keeping in mind that in the limiting case of extremely low temperature, $T \ll T_R$, the relative magnitude of the thermal correction is much less than a/R , the thermal effect in the Casimir force in this case should be considered as unobservable.

A completely different type of situation occurs under the condition $T \gg T_R$ which is well satisfied in all experiments on measuring the Casimir force performed at room temperature (we remind that for the sphere of $R = 100 \mu\text{m}$ radius $T_R = 11.4 \text{K}$). Here, irrespective of whether the inequality $T \ll T_a$ or $T \gg T_a$ is valid, the exact expression (41) leads in the zeroth order of the small parameter a/R to the simplified formulation of the PFA for the thermal correction to the Casimir force between a sphere and a plate [74]:

$$\Delta_T F_{\text{sp}}^{\text{exact}}(a, T) = 2\pi R \Delta_T \mathcal{F}_{\text{pp}}(a, T). \quad (44)$$

In the case $T \ll T_a$ the thermal correction to the Casimir free energy for two plane parallel plates, $\Delta_T \mathcal{F}_{\text{pp}}(a, T)$, is contained in Eq. (37):

$$\Delta_T \mathcal{F}_{\text{pp}}(a, T) = -\frac{\hbar c \zeta(3)}{16\pi a^3} \left(\frac{T}{T_a}\right)^3 \left(1 - \frac{T}{T_a}\right). \quad (45)$$

Thus, under a condition that $T \gg T_R$ the simplified formulation of the PFA is applicable not only to the total quantities $F_{\text{sp}}(a, T)$ and $\mathcal{F}_{\text{pp}}(a, T)$ [see Eq. (13)], but separately to the zero-temperature and thermal contributions to these quantities as well. This invalidates the statement of Ref. [66] that for a sphere above a plate at $T > T_R$ the PFA is inapplicable to each contribution alone made on the basis of the worldline approach.

V. APPLICABILITY OF THE PROXIMITY FORCE APPROXIMATION TO DESCRIBE THERMAL CORRECTION TO THE CASIMIR FORCE BETWEEN REAL METALS

Now we consider the possibility to apply the simplified formulation of the PFA for the theoretical description of the thermal correction to the Casimir force in recent experiments.

As noted in the Introduction, the thermal effect in the Casimir force is fundamentally different depending on what model of the dielectric permittivity of metal (Drude or plasma) is used. It is most straightforward to illustrate this difference in the low-temperature regime, $T \ll T_a$, for two plane parallel plates described by the simple plasma model [Eq. (16) with no contribution of core electrons, i.e., with $g_j = 0$] or the Drude model (15). In the case when the simple plasma model is used the temperature-dependent part of the free energy is given by [75]

$$\begin{aligned} \Delta_T \mathcal{F}_{pp}^{(p)}(a, T) = & -\frac{\hbar c}{8\pi a^3} \left\{ \frac{\zeta(3)}{3} \left(\frac{T}{T_a} \right)^3 - \frac{\pi^2}{90} \left(\frac{T}{T_a} \right)^4 \right. \\ & + \frac{\delta_0}{a} \left[\zeta(3) \left(\frac{T}{T_a} \right)^3 - \frac{2\pi^3}{45} \left(\frac{T}{T_a} \right)^4 \right] \\ & \left. - \left(\frac{\delta_0}{a} \right)^2 \zeta(5) \left(\frac{T}{T_a} \right)^5 \right\}, \end{aligned} \quad (46)$$

where $\delta_0 = 2\pi c/\omega_p$ is the effective skin depth in the frequency range of infrared optics. If, however, the Drude model is used under the condition $T \ll T_a$ one arrives at [16]

$$\begin{aligned} \Delta_T \mathcal{F}_{pp}^{(D)}(a, T) = & \Delta_T \mathcal{F}_{pp}^{(p)}(a, T) \\ & + \frac{k_B T \zeta(3)}{16\pi a^2} \left[1 - 4 \frac{\delta_0}{a} + 12 \left(\frac{\delta_0}{a} \right)^2 \right]. \end{aligned} \quad (47)$$

As is seen in Eq. (47), the additional term emerging in the case of the Drude model is positive and linear in temperature. Thus, it dominates at low temperatures leading to an anomalously large thermal correction. Note that the condition of low temperature with respect to T_a is satisfied in all modern experiments performed at room temperature at separations below $1 \mu\text{m}$. At the same time for all these experiments the condition of high temperature with respect to T_R , i.e., $T \gg T_R$, is satisfied. Because of this, it can be said [74] that modern experiments on measuring the Casimir force and its gradient in a sphere-plate configuration belong to the region of medium temperatures.

The measurement data of all experiments performed in the configuration of a rather large sphere in close proximity to a plane plate (i.e., under the condition $a \ll R$) were compared with the theory using the PFA. In static experiments (e.g., in Refs. [19, 31, 32, 52–55, 58–62]) Eq. (13) was used for this purpose. In dynamic experiments [19–23, 72, 73] the form of the PFA in Eq. (22) was employed. As was explained in Secs. II and III, in both cases

terms of order a/R , as compared with unity, were disregarded. This raises the question if this neglect imposes some constraints on the possibility to observe thermal effects in the Casimir force. Below we analyze this question using both theoretical approaches to the calculation of thermal Casimir force discussed in Sec. II.

We start with the Drude model approach using the tabulated optical data [68] for $\text{Im } \varepsilon(\omega)$ extrapolated to low frequencies by means of Eq. (15). The thermal effect can be characterized by the relative thermal correction to the Casimir force

$$\delta_T^{(D,1)}(a, T) = \frac{F_{\text{sp}}^{(D)}(a, T) - F_{\text{sp}}^{(D)}(a, 0)}{F_{\text{sp}}^{(D)}(a, T)} \quad (48)$$

and the Casimir pressure

$$\delta_T^{(D,2)}(a, T) = \frac{P^{(D)}(a, T) - P^{(D)}(a, 0)}{P^{(D)}(a, T)}. \quad (49)$$

We compute the relative correction (48) by Eqs. (5) and (13) over the separation region from 0.1 to 5 μm . The relative correction (49) is computed over the same separation region by using Eqs. (3) and (5). We remind that the measurement data for the quantity $P(a, T)$ in dynamic experiments are obtained by using Eq. (22) from the gradient of the Casimir force $\partial F_{\text{sp}}(a, T)/\partial a$ which in its turn was recalculated from the measured frequency shift. Thus, in static experiments using sphere-plate configuration, the PFA in the form of Eq. (13) is part of the theory, whereas in dynamic experiments the PFA in the form of Eq. (22) allows to convert the experimental data for the force gradient into the data for the equivalent Casimir pressure.

In Fig. 5 we present the computational results in percents for the relative thermal corrections $\delta_T^{(D,1)}$ (the solid line 1) and $\delta_T^{(D,2)}$ (the solid line 2) at $T = 300$ K as a function of separation in the region (a) from 0.1 to 5 μm and (b) from 0.1 to 1 μm . In the same figure, the short-dashed and long-dashed lines show the quantity a/R in percents taken with the same sign as the thermal corrections as a function of separation for $R = 100$ and 150 μm , respectively. These lines demonstrate the size of typical errors arising from the use of the PFA. As can be seen in Fig. 5, the relative thermal corrections for both the Casimir force and equivalent Casimir pressure are rather large. In the region from 1 to 4 μm they take negative values and achieve -35% and -47% , respectively. Within the separation region from 0.1 to 1 μm the magnitudes of thermal corrections to the force and to the pressure increase from 1.5% and 0.7% to 23% and 16%, respectively. In the same separation region

the error due to the use of the PFA varies from 0.1% to 1% for the sphere of 100 μm radius and from 0.07% to 0.7% for the sphere of 150 μm radius. Thus, the use of the PFA in the Drude model approach does not impose any constraints on the possibility to measure large thermal effects predicted in this approach.

The answer to the question whether or not the thermal corrections to the Casimir force in a sphere-plate configuration can be measured depends not only on the errors due to the application of the PFA, but also on the size of the total experimental error. Thus, in the static experiment [55] performed by means of an atomic force microscope the total relative experimental error of the Casimir force F_{sp} determined at a 60% confidence level at separations 100 and 200 nm is equal to 3.5% and 22.4%, respectively [76]. These are larger than the relative thermal correction $\delta_T^{(D,1)}$ in Fig. 5(b). Because of this, in the experiment of Refs. [55, 76] the predicted thermal correction cannot be either confirmed or excluded. A completely different type of situation occurs in dynamic experiments of Refs. [19–23] performed by means of a micromachined oscillator. Thus, in the most precise experiment of Refs. [22, 23] the total relative experimental error of the Casimir pressure P determined even at a higher, 95%, confidence level varies from 0.19% to 0.9% and to 9% when separation increases from 160 to 400 and to 750 nm, respectively. As can be seen in Fig. 5(b), the magnitude of the relative thermal correction $\delta_T^{(D,2)}$ remains much larger than the total experimental error over the entire range of experimental separations. That is the reason why, when no evidence of the predicted thermal corrections was found, Refs. [22, 23] arrived at the conclusion that the Drude model approach is experimentally excluded at a 95% confidence level (within a narrower separation region from 210 to 620 nm this approach was excluded at a 99.9% confidence level [23]).

It has been speculated in the literature that the experimental exclusion of the Drude model approach might be not warranted because of some theoretical and experimental uncertainties. Specifically, it was stressed [77] that the Drude parameters ω_p and γ used for the extrapolation of the optical data to low frequencies may vary. Besides, Ref. [78] surmised that measurements of absolute separations in Ref. [52] (which data were also used to exclude the Drude model approach) contain an unaccounted systematic error which could bring the data away from the theory. Here, we make a test of both these opportunities with respect to the theory-experiment comparison in Refs. [22, 23]. In Fig. 6 the differences between the theoretical Casimir pressures computed using the Drude model approach, as explained

above but with account of surface roughness, and the mean experimental Casimir pressures measured in Refs. [22, 23] are indicated as dots. The theoretical pressures for the lower set of dots are computed with the conventional Drude parameters of Sec. II ($\omega_p = 9.0$ eV, $\gamma = 0.035$ eV). The theoretical Casimir pressures for the upper set of dots are computed with the alternative Drude parameters [77], $\omega_p = 6.82$ eV, $\gamma = 0.0405$ eV, where the value of the plasma frequency is most different from the conventional one. The differences $P^{\text{theor}} - \bar{P}^{\text{expt}}$ with P^{theor} computed using all other alternative Drude parameters listed in Ref. [77] are sandwiched between the two sets of dots shown in Fig. 6. The solid lines in Fig. 6 indicate the borders of the confidence intervals $[-\Xi(a), \Xi(a)]$ computed in Ref. [23] at a 95% confidence level. By the construction of $[-\Xi(a), \Xi(a)]$, 95% of dots must belong to these intervals. However, as is seen in Fig. 6, almost all dots in both sets lie outside the solid lines demonstrating that the theoretical approach using the Drude model is excluded by the data at a 95% confidence level over the entire measurement range (as was mentioned above, within a bit narrower separation region the exclusion at a 99.9% confidence level holds). It is pertinent to note also that the use of optical data of Ref. [77] for the first absorption bands (which are slightly different from the data of Ref. [68] used in our computations) does not change this conclusion.

Now we consider the possibility to bring the experimental data in agreement with the Drude model approach by assuming that there is an unaccounted systematic error in the determination of absolute separations. Note that this systematic error (if any) is separation-independent. This is because in the setup used the differences between the values of separations where the Casimir pressures were measured are fixed interferometrically to high precision (see Ref. [20] for details). To find absolute separations, one should know the initial absolute separation which is determined from the electrostatic calibrations. If one admits that electrostatic calibrations contain some uncertainty, the initial separation would be burdened with some unaccounted constant systematic error which is translated to all separations. In an attempt to place the dots within the limits of the confidence intervals, in Fig. 7(a) we plot the differences $P^{\text{theor}} - \bar{P}^{\text{expt}}$ with two sets of the Drude parameters mentioned above as a function of separation, but with all separation distances decreased by $\Delta a = 1$ nm. (Note that the increase of separations results in even larger deviations of dots from the confidence intervals than in Fig. 6.) This corresponds to the assumption that an unaccounted systematic error in the measurement of separation distances in Refs. [22, 23] is

equal to 1 nm (remind that in actual fact the total error in the measurement of separations in Refs. [22, 23] is equal to 0.6 nm). As can be seen in Fig. 7(a), the shift of separations for 1 nm does not furnish the desired result for the lower set of dots at separations above 230 nm and is not helpful for the upper set of dots at any separation. The decrease of all separations for 3 nm [see Fig. 7(b)] expels the lower set from the confidence intervals at separations below 230 nm, but not yet includes these dots into the confidence interval at $a > 310$ nm. In Fig. 7(c) we illustrate the largest decrease of separations for 6 nm. Here, all dots related to the lower set are still outside the confidence intervals at $a > 430$ nm, but the dots of both sets are already outside of them at shortest separations. Note that similar to Fig. 6 the differences $P^{\text{theor}} - \bar{P}^{\text{expt}}$ computed with all other alternative Drude parameters are sandwiched between the two sets of dots shown in each of Figs. 7(a), 7(b), and 7(c). The same is correct when the optical data (not just the Drude parameters) from different sources are used. As shown in Ref. [79], the use of some alternative optical data instead of the data of Ref. [68] would decrease the magnitudes of theoretical Casimir pressures and, thus, only increase discrepancies between the predicted and experimental Casimir pressures. This means that no systematic error in the measurement of absolute separations can bring the experimental data of Refs. [22, 23] in agreement with the Drude model approach using any values of Drude parameters and any sets of the optical data.

From the above it follows that the sensitivity of dynamic experiments by means of micro-machined oscillator is quite sufficient to registrate the thermal correction to the Casimir pressure, as predicted by the Drude model approach. What is more, the application of the PFA in the form of Eq. (22) in this case is warranted because both the total quantities $\partial F_{\text{sp}}/\partial a$ and P and contained in them thermal corrections are much larger than a/R for the experimental parameters. The lack of any observation effect for the thermal correction to the Casimir pressure, as predicted by the Drude model approach, means that this approach is experimentally inconsistent.

We are coming now to the question is it possible to observe small thermal effect in the Casimir force, as predicted by the plasma model approach in sphere-plate configuration. In this case the relative thermal correction to the force, $\delta_T^{(p,1)}$, and to the pressure, $\delta_T^{(p,2)}$, are expressed once again by Eqs. (48) and (49) where $F_{\text{sp}}^{(D)}$ and $P^{(D)}$ are replaced with $F_{\text{sp}}^{(p)}$ and $P^{(p)}$ computed using the dielectric permittivity of the generalized plasma-like model (16). In Fig. 8 the computational results (in percents) are presented for $\delta_T^{(p,1)}$ (the solid

line 1) and for $\delta_T^{(p,2)}$ (the solid line 2) at $T = 300$ K as a function of a in the region (a) from 0.1 to $5 \mu\text{m}$ and (b) from 0.1 to $1 \mu\text{m}$. The short-dashed and long-dashed lines show the quantity a/R (in percents) for $R = 100$ and $150 \mu\text{m}$, respectively. As can be seen in Fig. 8, the thermal corrections computed using the plasma model approach are positive and increase monotonously with the increase of separation. At $a < 1 \mu\text{m}$ their magnitudes are much less than the magnitudes of the thermal corrections computed using the Drude model approach (see Fig. 5). As a result, $\delta_T^{(p,1)}$ lies below the short-dashed line related to the static experiments. The relative correction to the Casimir pressure, $\delta_T^{(p,2)}$, lies below the long-dashed line related to the dynamic experiments at $a < 1.6 \mu\text{m}$. This means that one cannot attribute physical meaning to such small values of the thermal corrections $\delta_T^{(p,1)}$ and $\delta_T^{(p,2)}$ computed using the PFA [Eqs. (13) and (22)] which disregards contributions to the force and to the pressure of order a/R .

The magnitudes of the thermal corrections $\delta_T^{(p,1)}$ and $\delta_T^{(p,2)}$ are markedly larger than a/R shown by the short-dashed (long-dashed) lines only at separations $a > 0.6 \mu\text{m}$ ($a > 2 \mu\text{m}$). However, either in the static experiment [55] on measuring the Casimir force F_{sp} or in the most precise dynamic experiment [22, 23] on measuring the Casimir pressure P , over the entire separations regions $a \geq 0.1 \mu\text{m}$ and $a \geq 0.16 \mu\text{m}$, the magnitudes of $\delta_T^{(p,1)}$ and $\delta_T^{(p,2)}$ fall far short of the total relative experimental error. It is not surprising, then, that thermal effects were not observed in these experiments. One more possibility for future measurements is to use spheres of larger radius. This allows to make a/R smaller and, thus, make thermal corrections $\delta_T^{(p,1)}$ and $\delta_T^{(p,2)}$ computed using the PFA physically meaningful over the entire range of separations $a \geq 0.1 \mu\text{m}$. In addition, in static experiments the Casimir force F_{sp} is larger for a sphere of larger R resulting in a smaller relative experimental error. For spheres of centimeter-size radii, however, unavoidable deviations from perfect spherical shape is a problem of great concern which prevents accurate electrostatic calibration [80]. It is therefore unlikely that small thermal effect in the Casimir force, as predicted by the plasma model approach, will be observed in the configuration of a sphere above a plate.

We conclude this section with a brief discussion of recent exact results for the thermal Casimir force between a sphere and a plate described by simple plasma and Drude models without account for interband transitions of core electrons [25] and by the generalized plasma-like and Drude-like models [26]. The key question is whether or not these results support computations performed using the PFA. As was discussed in Sec. IV, for ideal met-

als the exact results in the zeroth order in a/R coincide with the PFA if $T \gg T_R$. This is the case for both the total Casimir force or Casimir pressure and separately for the thermal corrections. Unfortunately, the exact computations of Refs. [25, 26] were performed in regions far away from the values of experimental parameters and outside the region where the PFA is applicable. For example, in Ref. [25] the sphere radii were chosen to be $R = 0.1, 0.2, 0.5, 1, 2, 5 \mu\text{m}$ and computations were performed at separations from 0.5 to $10 \mu\text{m}$. For a sphere radius $R = 10 \mu\text{m}$ the computations of Ref. [25] were made from $a = 1$ to $10 \mu\text{m}$. Thus, in all cases considered it holds $a/R \geq 0.1$. Remind that for the experimental parameters of Refs. [55, 76] a/R varies from 0.00063 to 0.003 and for the parameters of Refs. [22, 23] from 0.0011 to 0.005.

According to the results presented in Secs. II and III, the PFA in the form of Eqs. (13) and (22) is applicable only at $a/R \ll 1$. Because of this, the speculation of Ref. [25] that at small separations the Drude and plasma models lead to Casimir force values much closer than predicted by the PFA made on the basis of computations in the region of $a/R > 0.1$ is unjustified. The computational results of Ref. [25] at $a = 0.5 \mu\text{m}$, $T = 300 \text{ K}$ clearly demonstrate that deviations between the exact theory and the PFA vanish with decreasing a/R . Thus, from Fig. 3 of Ref. [25] it can be seen that relative deviation of the quantity $F_{\text{sp}}^{(p)}(a, T)/F_{\text{sp}}^{(D)}(a, T)$ computed exactly from that computed using the PFA decreases from 9.2% to 2.5% when the sphere radius increases from $R = 0.1 \mu\text{m}$ ($a/R = 5$) to $R = 5 \mu\text{m}$ ($a/R = 0.1$). In such a manner exact computations confirm that the computational error in the ratio $F_{\text{sp}}^{(p)}(a, T)/F_{\text{sp}}^{(D)}(a, T)$ arising from using the PFA for real metals (0.025 for $a/R = 0.1$) is smaller than a/R . For the experimental values of a/R mentioned above this error would be much less than the total experimental error. Because of this it can be stated with certainty that the comparison of the performed experiments with the exact theory instead of the PFA (when the exact will become available) will not lead to any changes with respect to already obtained conclusions.

Both papers [25, 26] claim that for large separations in the sphere-plane geometry the Drude model leads to a force a factor of 3/2 smaller than the plasma model (instead of a factor of 2 as it holds for two parallel metal plates). In such a general form this formulation is, however, somewhat misleading as it does not cover all relevant limiting cases. In fact it is correct only in the case when $\lambda_p = 2\pi c/\omega_p \ll R \ll a$ [25, 26], i.e., outside the application region of the PFA. If, however, we consider large separations $a \gg \hbar c/(2k_B T)$, i.e., $T \gg$

T_a , and large sphere $R \gg a$ (which means that the PFA is applicable), then the exactly calculated ratio $F_{\text{sp}}^{(p)}/F_{\text{sp}}^{(D)} = 2$. The same result is obtained using the PFA. As shown in Ref. [26] by means of exact computations, there is one more limiting case, $a \gg R$, $R \leq \lambda_p$ and $T \gg T_a$, where $F_{\text{sp}}^{(p)}/F_{\text{sp}}^{(D)} = 1$. This result is quite natural because a small sphere above a plate can be modelled as an atom characterized by some effective dynamic polarizability [81]. Keeping in mind that at large separations only the static polarizability is relevant which is common for the plasma and Drude models, both the free energies and forces computed using these models coincide in the limit of large a . Thus, in sphere-plate geometry the ratio $F_{\text{sp}}^{(p)}/F_{\text{sp}}^{(D)}$ can take different values, $3/2$, 2 , and 1 , in the large distance limit depending on the parameters of the problem. In the experimental situations, however, where $a \ll R$ and $R \gg \lambda_p$, in the limit of large distances, $a \gg \hbar c/(2k_B T)$, it holds $F_{\text{sp}}^{(p)}/F_{\text{sp}}^{(D)} = 2$ like for two parallel plates.

In Ref. [26] the exact computations of the free energies $\mathcal{F}_{\text{sp}}^{(p)}$ and $\mathcal{F}_{\text{sp}}^{(D)}$ were performed for a sphere of $R = 5 \mu\text{m}$ radius at $T = 300 \text{ K}$ and 77 K within the separation region from 0.265 to $95 \mu\text{m}$. This corresponds to the values of a/R varying from 0.053 to 19 . Once again, only near the smallest a/R considered the PFA becomes applicable, whereas for the comparison with recent experiments more than one order of magnitude smaller ratios a/R are required. At the shortest separation $a = 0.265 \mu\text{m}$ ($a/R = 5.3\%$) from Fig. 5 of Ref. [26] one obtains the exact value for the ratio $\mathcal{F}_{\text{sp}}^{(p)}/\mathcal{F}_{\text{sp}}^{(D)} = 1.11$ at $T = 300 \text{ K}$. The same ratio computed using the PFA is equal to 1.14 leading to a relative 2.6% deviation between the PFA and exact results which is less than one half of a/R . This confirms that for real metals in sphere-plate geometry the PFA results for both the thermal Casimir force and free energy go to the respective exact results with decreasing a/R .

VI. THE POSSIBILITY TO MEASURE THERMAL EFFECT IN THE GRADIENT OF THE CASIMIR PRESSURE

The original Casimir configuration of two parallel plates is the only one where the comparison of experiment with theory does not require either the PFA or more sophisticated exact computational methods which can be effectively used so far solely in some restricted ranges of parameters. The only experiment of this kind was performed [82] in the modern stage of the Casimir force measurements. This is an experiment of dynamic type where one

of the plates was oscillating at the natural oscillator frequency. As a result, the shift of this frequency under the influence of the Casimir pressure was measured and recalculated into the gradient of the Casimir pressure. The experiment [82] reported 15% measure of agreement between the data and theory using the model of ideal metals (see review [11] for details).

The gradient of the Casimir pressure

$$P'(a, T) \equiv \frac{\partial P(a, T)}{\partial a} \quad (50)$$

is obtained from Eqs. (3) and (5) by differentiation with respect to separation

$$P'(a, T) = \frac{2k_B T}{\pi} \sum_{l=0}^{\infty} \int_0^{\infty} q_l^2 k_{\perp} dk_{\perp} \sum_{\alpha} \frac{r_{\alpha}^2 e^{-2q_l a}}{(1 - r_{\alpha}^2 e^{-2q_l a})^2}. \quad (51)$$

The thermal correction to the gradient of the Casimir pressure can be characterized by the quantity

$$\delta_T^{(3)}(a, T) = \frac{P'(a, T) - P'(a, 0)}{P'(a, T)}. \quad (52)$$

We will add additional indices D , p and IM and calculate the quantities $\delta_T^{(D,3)}$, $\delta_T^{(p,3)}$ and $\delta_T^{(IM,3)}$ depending on the used model of dielectric properties of metal described in Sec. II.

The computational results for the relative thermal correction (52) to the gradient of the Casimir pressure as a function of separation at $T = 300$ K are presented in Fig. 9. Here, the separation region from 0.5 to 5 μm is considered because at shorter separations it would be hard to experimentally keep the plates parallel. The dashed, solid, and dotted lines represent results computed by using the tabulated optical data extrapolated to low frequencies by the Drude model with conventional parameters, the generalized plasma-like model, and the model of ideal metals, respectively. As can be seen in Fig. 9, for ideal metal plates and plates described by the generalized plasma-like model the relative thermal correction to the gradient of the Casimir pressure monotonously increases with the increase of separation. At separations $a \leq 3 \mu\text{m}$, where the experiment is feasible, $\delta_T^{(p,3)} \leq 3.6\%$ and $\delta_T^{(IM,3)} \leq 1.3\%$. So small magnitudes of $\delta_T^{(p,3)}$ make it impossible to observe the thermal corrections due to the generalized plasma-like model in the measurements of the gradient of the Casimir pressure. By contrast, the relative thermal correction $\delta_T^{(D,3)}$ computed using the Drude model approach decreases monotonously with increase of separation from 0.5 to 4.1 μm where it achieves the minimum value of -53.3% . At $a = 3 \mu\text{m}$ it holds $\delta_T^{(D,3)} = -43\%$.

Thus, the proposed experiment on measuring the gradient of the Casimir pressure [83] might provide one more confirmation for the exclusion of the Drude model approach, but is not well adapted for the measurement of the thermal correction, as predicted by the generalized plasma-like model. Note that according to the authors of Ref. [83] their effort to measure the Casimir force is not yet successful due to the use of Al surfaces. The point is that Al is the subject of quick oxidation even in high vacuum. For this reason, in the first precise measurement of the Casimir force [53], Al surfaces were coated with thin transparent layers of Au/Pd. The use of such layers, however, complicates the comparison between experiment and theory. As a result, starting from 2000 almost all experiments on the Casimir force between metallic test bodies [11] used Au coated surfaces. Presently another setup with parallel Au surfaces, instead of Al, is under construction [83].

It can be shown also analytically that measurements of the gradient of the Casimir pressure are unsuitable for the detection of small thermal corrections. For example, for ideal metal plates in the limit of low temperatures $T \ll T_a$ it holds [6]

$$P^{(IM)}(a, T) = -\frac{\pi^2 \hbar c}{240a^4} \left[1 + \frac{1}{3} \left(\frac{T}{T_a} \right)^4 - \frac{120}{\pi} \frac{T}{T_a} e^{-2\pi T_a/T} \right]. \quad (53)$$

Taking into account that the second contribution on the right-hand side of Eq. (53) does not depend on separation, the main contribution to the gradient of the Casimir pressure in the low-temperature limit takes the form

$$\frac{\partial P^{(IM)}(a, T)}{\partial a} = \frac{\pi^2 \hbar c}{60a^5} (1 + 60e^{-2\pi T_a/T}). \quad (54)$$

As can be seen on the right-hand side of Eq. (54), there are no terms in powers of T/T_a and the thermal correction is exponentially small. Equation (54) reproduces the exactly calculated $\partial P^{(IM)}(a, T)/\partial a$ at $T = 300$ K with an error of less than 1% up to the separation distance $a = 3 \mu\text{m}$. The absence of power-type thermal corrections in the gradient of the Casimir pressure for ideal metals explains why the thermal effect in this case is so small.

At low temperatures, the analytical representation for the gradient of the Casimir pressure can be obtained for real metals as well. Thus, for metals described by the generalized plasma-like model at separations above $0.5 \mu\text{m}$ considered here the influence of interband transitions can be neglected. Then the thermal correction in the gradient of the Casimir pressure is

obtained as the negative second derivative of Eq. (46) leading to

$$\begin{aligned} \frac{\partial P^{(p)}(a, T)}{\partial a} = \frac{\pi^2 \hbar c}{60a^5} & \left[1 - \frac{20}{3} \frac{\delta_0}{a} + 36 \left(\frac{\delta_0}{a} \right)^2 \right. \\ & \left. + \frac{15\zeta(3)}{\pi^3} \frac{\delta_0}{a} \left(\frac{T}{T_a} \right)^3 \right], \end{aligned} \quad (55)$$

where the exponentially small terms are omitted. Here, the leading thermal correction is of power-type, but it contains the first and third power of small parameters. Equation (55) provides a better than 1% approximation for the exactly computed $\partial P^{(p)}(a, T)/\partial a$ over the range of separations below $1.3 \mu\text{m}$. Similar low-temperature results for metals described by the Drude model can be obtained by calculating the negative second derivative of Eq. (47)

$$\frac{\partial P^{(D)}(a, T)}{\partial a} = \frac{\partial P^{(p)}(a, T)}{\partial a} - \frac{3k_B T \zeta(3)}{8\pi a^4} \left(1 - 8 \frac{\delta_0}{a} + 40 \frac{\delta_0^2}{a^2} \right) \quad (56)$$

This approximate expression reproduces the values of $\partial P^{(D)}(a, T)/\partial a$ with an error less than 1% at separations below $1 \mu\text{m}$.

To conclude this section, for the configuration of two parallel plates in the dynamic regime the relative thermal correction to the gradient of the Casimir pressure computed using the plasma model approach achieves 20% only at $a = 5 \mu\text{m}$ (see Fig. 9). The same relative size of the thermal correction computed using the plasma model but to the Casimir pressure is achieved at a shorter separation $a = 3.7 \mu\text{m}$ [see the solid line 2 Fig. 8(a)]. Thus, the static experiment with two parallel plates of sufficiently large area might be preferable for the registration of small thermal corrections at relatively large separations. Although at the same separation the relative thermal correction to the Casimir force in a sphere-plate configuration is larger [43% in accordance with the solid line 1 in Fig. 8(a) at $a = 3.7 \mu\text{m}$], small values of forces for spheres of relatively small radii make its measurement impossible. As was discussed above, the use of centimeter-size spheres meets difficulties due to unavoidable deviations from sphericity. In this respect the increase of plate area and, thus, the increase of the Casimir force, may make possible to decrease the experimental error at separations of a few micrometers to about 10%, i.e., below the characteristic size of small thermal effect predicted by the plasma model approach.

VII. CONCLUSIONS AND DISCUSSION

In the foregoing we have analyzed the possibility to measure thermal effects in the Casimir force between metals in the configurations of a sphere above a plate and two parallel plates. In connection with the sphere-plate configuration, a detailed study of the reliability of the PFA to describe the thermal Casimir force was performed. We have considered the two formulations of the PFA, the most general, Derjaguin, formulation [49] and the simplified formulation of Ref. [24] which was used for the comparison of many experiments on the measuring of the Casimir force with theory. We show in Sec. II that for a large sphere, i.e., under the condition $a \ll R$, the magnitude of the relative difference between thermal Casimir forces F_{sp} computed for real metals by using the two formulations of the PFA is less than a/R . This holds regardless of what approach to the description of charge carriers (Drude or plasma model) is employed. A similar result is obtained in Sec. III for the gradient of the thermal Casimir force in sphere-plate configuration, $\partial F_{\text{sp}}/\partial a$. Here again the relative difference computed using the two formulations is less than a/R . The obtained results are compared with the experimental data of Ref. [72] demonstrating that for large spheres of different radii at $T = 300$ K the relative differences of the measured $|F_{\text{sp}}|$, $\partial F_{\text{sp}}/\partial a$ and those computed using the simplified formulation of the PFA are also less than a/R . From this we can conclude that the simplified formulation of the PFA is a good approximation for the calculation of thermal Casimir forces in sphere-plate configuration for spheres of large radii.

In Sec. IV special attention is paid to the case of an ideal metal sphere above an ideal metal plate. In this case a simple analytic expression for the difference between the two formulations of the PFA is obtained. The thermal correction to the Casimir force computed using the PFA is considered both in the limiting case of very low temperatures, $T \ll T_R$, and in the case $T \gg T_R$. The latter includes the region of parameters where all measurements of the Casimir force in sphere-plate configuration have been performed. The results for the thermal correction obtained using the PFA are compared with available exact results. It is emphasized that in the experimental region $T \gg T_R$ the exact results of Ref. [74] in the zeroth order of a/R coincide with the simplified formulation of the PFA. This provides a theoretical basis for the application of the PFA in the measurements of the thermal Casimir force for the comparison between experiment and theory.

The applicability of the PFA and the possibility to observe the thermal correction to

the Casimir force in the configuration of a sphere above a plate made of real metals are discussed in Sec. V. Here, the relative thermal corrections to the Casimir force and to the Casimir pressure are computed in the framework of both the Drude model and the plasma model approaches. The obtained results are compared with the error introduced from the use of the PFA and with typical experimental errors of force and pressure measurements. New evidence is provided that some unaccounted systematic errors in the experiment of Refs. [22, 23] cannot bring the measurement results in agreement with the prediction of the Drude model approach. It is argued that the configuration of a sphere above a plate is well suited to exclude the large thermal correction derived within the Drude model approach but scarcely can be used for the experimental observation of small thermal effects, as predicted from the plasma model approach. The reason is that the respective thermal correction $\delta_T^{(p)}$ is several times larger than the error of PFA, a/R , only at sufficiently large separations, where the error of force or equivalent pressure measurements exceeds $\delta_T^{(p)}$. The exact computational results for the thermal correction to the Casimir force between real metals described by the Drude and plasma models are compared with the PFA results. It is shown that the region of parameters where the exact results are available is outside the area of application of the PFA. We demonstrate that at relatively large separations the ratio $F_{\text{sp}}^{(p)}/F_{\text{sp}}^{(D)}$ can go to different limiting values (2, 3/2 or 1) depending on the relationship between the parameters a , R , λ_p and T . This generalizes the results of Refs. [25, 26]. The performed comparison enables us to conclude that the available exact results for real metals converge to the PFA results when $a/R \rightarrow 0$. For the experimental values of a/R varying from 0.00063 to 0.005 the errors due to the use of the PFA instead of the exact methods are much less than the experimental error of force and pressure measurements in all experiments performed to the present day.

In the configuration of two parallel plates, we have calculated the relative thermal correction to the gradient of the Casimir pressure which is measured in the dynamic regime (Sec. VI). We show that a small thermal effect, as predicted in the plasma model approach, is additionally suppressed in the gradient of the Casimir pressure. Because of this, the original Casimir configuration of two parallel plates of sufficiently large area used in the static regime remains the most prospective for measurement of small thermal effect in the Casimir force.

Acknowledgments

The authors acknowledge helpful discussions with M. Bordag. G.L.K. and V.M.M. are grateful to the Institute for Theoretical Physics, Leipzig University, where this work was performed, for kind hospitality. They were supported by Deutsche Forschungsgemeinschaft, Grant No. GE 696/10–1. G.L.K. was also supported by the Grant of the Russian Ministry of Education P–184.

-
- [1] H. B. G. Casimir, *Proc. K. Ned. Akad. Wet.* **51**, 793 (1948).
 - [2] P. W. Milonni, *The Quantum Vacuum* (Academic Press, San Diego, 1994).
 - [3] V. M. Mostepanenko and N. N. Trunov, *The Casimir Effect and its Applications* (Clarendon, Oxford, 1997).
 - [4] M. Krech, *The Casimir Effect in Critical Systems* (World Scientific, Singapore, 1994).
 - [5] K. A. Milton, *The Casimir Effect* (World Scientific, Singapore, 2001).
 - [6] M. Bordag, G. L. Klimchitskaya, U. Mohideen, and V. M. Mostepanenko, *Advances in the Casimir Effect* (Oxford University Press, Oxford, 2009).
 - [7] E. M. Lifshitz, *Zh. Eksp. Teor. Fiz.* **29**, 94 (1956) [*Sov. Phys. JETP* **2**, 73 (1956)].
 - [8] I. E. Dzyaloshinskii, E. M. Lifshitz, and L. P. Pitaevskii, *Usp. Fiz. Nauk* **73**, 381 (1961) [*Adv. Phys.* **10**, 165 (1961)].
 - [9] T. Emig, N. Graham, R. L. Jaffe, and M. Kardar, *Phys. Rev. D* **77**, 025005 (2008).
 - [10] O. Kenneth and I. Klich, *Phys. Rev. B* **78**, 014103 (2008).
 - [11] G. L. Klimchitskaya, U. Mohideen, and V. M. Mostepanenko, *Rev. Mod. Phys.* **81**, 1827 (2009).
 - [12] M. Boström and B. E. Sernelius, *Phys. Rev. Lett.* **84**, 4757 (2000).
 - [13] M. Bordag, B. Geyer, G. L. Klimchitskaya, and V. M. Mostepanenko, *Phys. Rev. Lett.* **85**, 503 (2000).
 - [14] C. Genet, A. Lambrecht, and S. Reynaud, *Phys. Rev. A* **62**, 012110 (2000).
 - [15] V. B. Bezerra, G. L. Klimchitskaya, and V. M. Mostepanenko, *Phys. Rev. A* **66**, 062112 (2002).
 - [16] V. B. Bezerra, G. L. Klimchitskaya, V. M. Mostepanenko, and C. Romero, *Phys. Rev. A* **69**,

- 022119 (2004).
- [17] J. S. Høye, I. Brevik, S. A. Ellingsen, and J. B. Aarseth, *Phys. Rev. E* **75**, 051127 (2007).
 - [18] I. Brevik, S. A. Ellingsen, J. S. Høye, and K. A. Milton, *J. Phys. A: Math. Theor.* **41**, 164017 (2008).
 - [19] R. S. Decca, E. Fischbach, G. L. Klimchitskaya, D. E. Krause, D. López, and V. M. Mostepanenko, *Phys. Rev. D* **68**, 116003 (2003).
 - [20] R. S. Decca, D. López, E. Fischbach, G. L. Klimchitskaya, D. E. Krause, and V. M. Mostepanenko, *Ann. Phys. (N.Y.)* **318**, 37 (2005).
 - [21] G. L. Klimchitskaya, R. S. Decca, E. Fischbach, D. E. Krause, D. López, and V. M. Mostepanenko, *Int. J. Mod. Phys. A* **20**, 2205 (2005).
 - [22] R. S. Decca, D. López, E. Fischbach, G. L. Klimchitskaya, D. E. Krause, and V. M. Mostepanenko, *Phys. Rev. D* **75**, 077101 (2007).
 - [23] R. S. Decca, D. López, E. Fischbach, G. L. Klimchitskaya, D. E. Krause, and V. M. Mostepanenko, *Eur. Phys. J. C* **51**, 963 (2007).
 - [24] J. Blocki, J. Randrup, W. J. Swiatecki, and C. F. Tsang, *Ann. Phys. (N.Y.)* **105**, 427 (1977).
 - [25] A. Canaguier-Durand, P. A. Maia Neto, A. Lambrecht, and S. Reynaud, *Phys. Rev. Lett.* **104**, 040403 (2010).
 - [26] R. Zandi, T. Emig, and U. Mohideen, *Phys. Rev. B* **81**, 195423 (2010).
 - [27] B. Geyer, G. L. Klimchitskaya, and V. M. Mostepanenko, *Phys. Rev. D* **72**, 085009 (2005).
 - [28] B. Geyer, G. L. Klimchitskaya, and V. M. Mostepanenko, *Int. J. Mod. Phys. A* **21** 5007 (2006).
 - [29] G. L. Klimchitskaya, B. Geyer, and V. M. Mostepanenko, *J. Phys. A* **39**, 6495 (2006).
 - [30] B. Geyer, G. L. Klimchitskaya, and V. M. Mostepanenko, *Ann. Phys. (N.Y.)* **323**, 291 (2008).
 - [31] F. Chen, G. L. Klimchitskaya, V. M. Mostepanenko, and U. Mohideen, *Optics Express* **15**, 4823 (2007).
 - [32] F. Chen, G. L. Klimchitskaya, V. M. Mostepanenko, and U. Mohideen, *Phys. Rev. B* **76**, 035338 (2007).
 - [33] J. M. Obrecht, R. J. Wild, M. Antezza, L. P. Pitaevskii, S. Stringari, and E. A. Cornell, *Phys. Rev. Lett.* **98**, 063201 (2007).
 - [34] G. L. Klimchitskaya and V. M. Mostepanenko, *J. Phys. A: Math. Theor.* **41**, 312002(F) (2008).
 - [35] L. P. Pitaevskii, *Phys. Rev. Lett.* **101**, 163202 (2008).
 - [36] D. A. R. Dalvit and S. K. Lamoreaux, *Phys. Rev. Lett.* **101**, 163203 (2008).

- [37] B. Geyer, G. L. Klimchitskaya, U. Mohideen, and V. M. Mostepanenko, Phys. Rev. Lett. **102**, 189301 (2009).
- [38] L. P. Pitaevskii, Phys. Rev. Lett. **102**, 189302 (2009).
- [39] R. S. Decca, E. Fischbach, B. Geyer, G. L. Klimchitskaya, D. E. Krause, D. López, U. Mohideen, and V. M. Mostepanenko, Phys. Rev. Lett. **102**, 189303 (2009).
- [40] D. A. R. Dalvit and S. K. Lamoreaux, Phys. Rev. Lett. **102**, 189304 (2009).
- [41] V. M. Mostepanenko, R. S. Decca, E. Fischbach, B. Geyer, G. L. Klimchitskaya, D. E. Krause, D. López, and U. Mohideen, Int. J. Mod. Phys. A **24**, 1721 (2009).
- [42] D. A. R. Dalvit and S. K. Lamoreaux, J. Phys.: Conf. Series **161**, 012009 (2009).
- [43] B. E. Sernelius, Phys. Rev. A **80**, 043828 (2009).
- [44] F. Intravaia and C. Henkel, Phys. Rev. Lett. **103**, 130405 (2009).
- [45] P. R. Buenzli and Ph. A. Martin, Phys. Rev. E **77**, 011114 (2008).
- [46] G. Bimonte, Phys. Rev. A **79**, 042107 (2009).
- [47] F. Cornu and Ph. A. Martin, J. Phys. A: Math. Theor. **42**, 495001 (2009).
- [48] V. M. Mostepanenko and G. L. Klimchitskaya, Int. J. Mod. Phys. A **25**, 2302 (2010).
- [49] B. V. Derjaguin, Kolloid. Z. **69**, 155 (1934).
- [50] B. E. Sernelius and C. E. Román-Velázquez, Phys. Rev. A **78**, 032111 (2008).
- [51] E. M. Lifshitz and L. P. Pitaevskii, *Statistical Physics*, Part. II (Pergamon Press, Oxford, 1980).
- [52] S. K. Lamoreaux, Phys. Rev. Lett. **78**, 5 (1997).
- [53] U. Mohideen and A. Roy, Phys. Rev. Lett. **81**, 4549 (1998).
- [54] A. Roy, C.-Y. Lin, and U. Mohideen, Phys. Rev. D **60**, 111101(R) (1999).
- [55] B. W. Harris, F. Chen, and U. Mohideen, Phys. Rev. A **62**, 052109 (2000).
- [56] H. B. Chan, V. A. Aksyuk, R. N. Kleiman, D. J. Bishop, and F. Capasso, Science, **291**, 1941 (2001).
- [57] H. B. Chan, V. A. Aksyuk, R. N. Kleiman, D. J. Bishop, and F. Capasso, Phys. Rev. Lett. **87**, 211801 (2001).
- [58] F. Chen, G. L. Klimchitskaya, U. Mohideen, and V. M. Mostepanenko, Phys. Rev. Lett. **88**, 101801 (2002).
- [59] F. Chen, G. L. Klimchitskaya, U. Mohideen, and V. M. Mostepanenko, Phys. Rev. A **66**, 032113 (2002).

- [60] F. Chen, G. L. Klimchitskaya, V. M. Mostepanenko, and U. Mohideen, *Phys. Rev. Lett.* **97**, 170402 (2006).
- [61] H.-C. Chiu, G. L. Klimchitskaya, V. N. Marachevsky, V. M. Mostepanenko, and U. Mohideen, *Phys. Rev. B* **80**, 121402(R) (2009).
- [62] H.-C. Chiu, G. L. Klimchitskaya, V. N. Marachevsky, V. M. Mostepanenko, and U. Mohideen, *Phys. Rev. B* **81**, 115417 (2010).
- [63] R. S. Decca, E. Fischbach, G. L. Klimchitskaya, D. E. Krause, D. López, and V. M. Mostepanenko, *Phys. Rev. D* **79**, 124021 (2009).
- [64] A. Scardicchio and R. L. Jaffe, *Nucl. Phys. B* **704**, 552 (2005).
- [65] H. Gies and K. Klingmüller, *Phys. Rev. D* **74**, 045002 (2006).
- [66] A. Weber and H. Gies, arXiv:1003.3420v1.
- [67] E. Fischbach, G. L. Klimchitskaya, D. E. Krause, and V. M. Mostepanenko, *Eur. Phys. J. C* **68**, 223 (2010).
- [68] *Handbook of Optical Constants of Solids*, ed. E. D. Palik (Academic, New York, 1985).
- [69] A. Lambrecht and S. Reynaud, *Eur. Phys. J. D* **8**, 309 (2000).
- [70] V. B. Svetovoy and R. Esquivel, *Phys. Rev. E* **72**, 036113 (2005).
- [71] B. E. Sernelius, *Phys. Rev. B* **71**, 235114 (2005).
- [72] D. E. Krause, R. S. Decca, D. López, and E. Fischbach, *Phys. Rev. Lett.* **98**, 050403 (2007).
- [73] G. Jourdan, A. Lambrecht, F. Comin, and J. Chevrier, *Europhys. Lett.* **85**, 31001 (2009).
- [74] M. Bordag and I. Pirozhenko, *Phys. Rev. D* **81**, 085023 (2010).
- [75] B. Geyer, G. L. Klimchitskaya, and V. M. Mostepanenko, *Int. J. Mod. Phys. A* **16**, 3291 (2001).
- [76] F. Chen, G. L. Klimchitskaya, U. Mohideen, and V. M. Mostepanenko, *Phys. Rev. A* **69**, 022117 (2004).
- [77] V. B. Svetovoy, P. J. van Zwol, G. Palasantzas, and J. Th. M. De Hosson, *Phys. Rev. B* **77**, 035439 (2008).
- [78] W. J. Kim, A. O. Sushkov, D. A. R. Dalvit, and S. K. Lamoreaux, *Phys. Rev. A* **81**, 022505 (2010).
- [79] B. Geyer, G. L. Klimchitskaya, and V. M. Mostepanenko, *Phys. Rev. B* **81**, 245421 (2010).
- [80] R. S. Decca, E. Fischbach, G. L. Klimchitskaya, D. E. Krause, D. López, U. Mohideen, and V. M. Mostepanenko, *Phys. Rev. A* **79**, 026101 (2009).

- [81] J. F. Babb, G. L. Klimchitskaya, and V. M. Mostepanenko, Phys. Rev. A **70**, 042901 (2004).
 [82] G. Bressi, G. Carugno, R. Onofrio, and G. Ruoso, Phys. Rev. Lett. **88**, 041804 (2002).
 [83] P. Antonini, G. Bimonte, G. Bressi, G. Carugno, G. Galeazzi, G. Messineo, and G. Ruoso, J. Phys.: Conf. Ser. **161**, 012006 (2009).

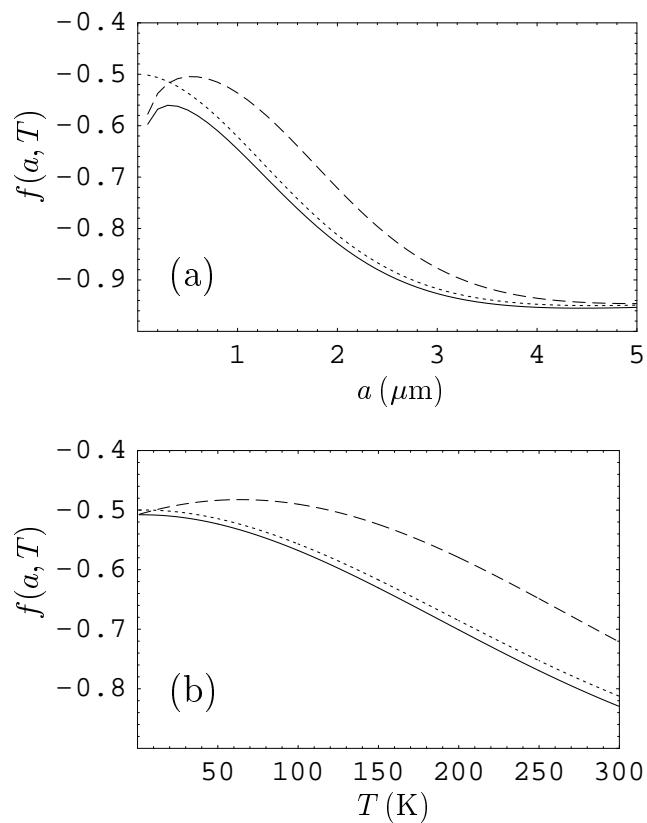


FIG. 1: The quantity f characterizing differences between the two formulations of the PFA for the Casimir force as a function of (a) separation at room temperature $T = 300$ K and (b) temperature at a separation $a = 2 \mu\text{m}$. The dotted, dashed and solid lines show the results computed using ideal metals, Drude and plasma model approaches, respectively. The sphere radius $R = 100 \mu\text{m}$.

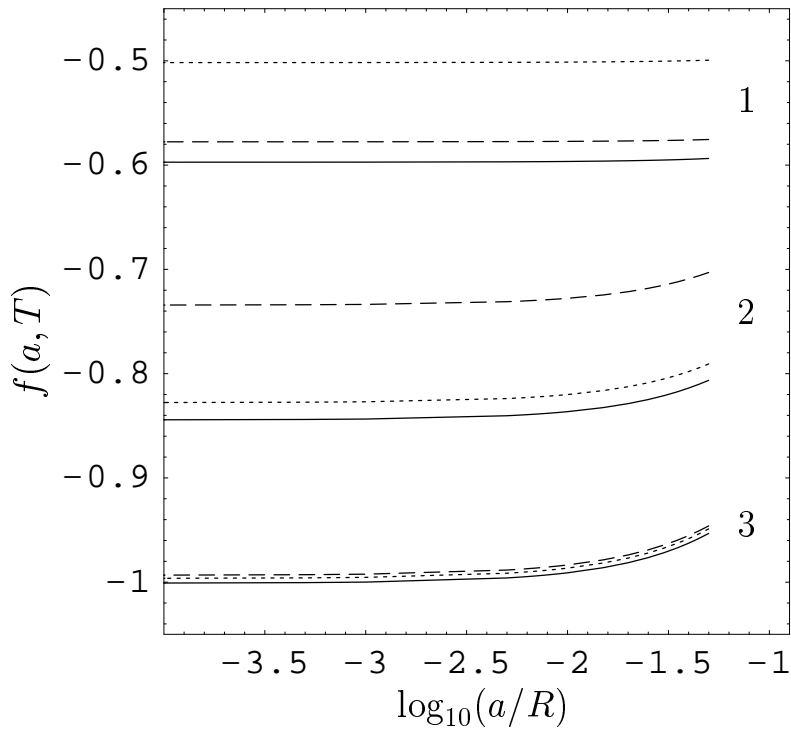


FIG. 2: The quantity f characterizing differences between the two formulations of the PFA for the Casimir force as a function of a/R at room temperature $T = 300$ K. The dotted, dashed and solid lines show the results computed using ideal metals, Drude and plasma model approaches, respectively. The groups of lines numerated 1, 2, and 3 are for the respective fixed separations $a = 0.1, 2, \text{ and } 5 \mu\text{m}$.

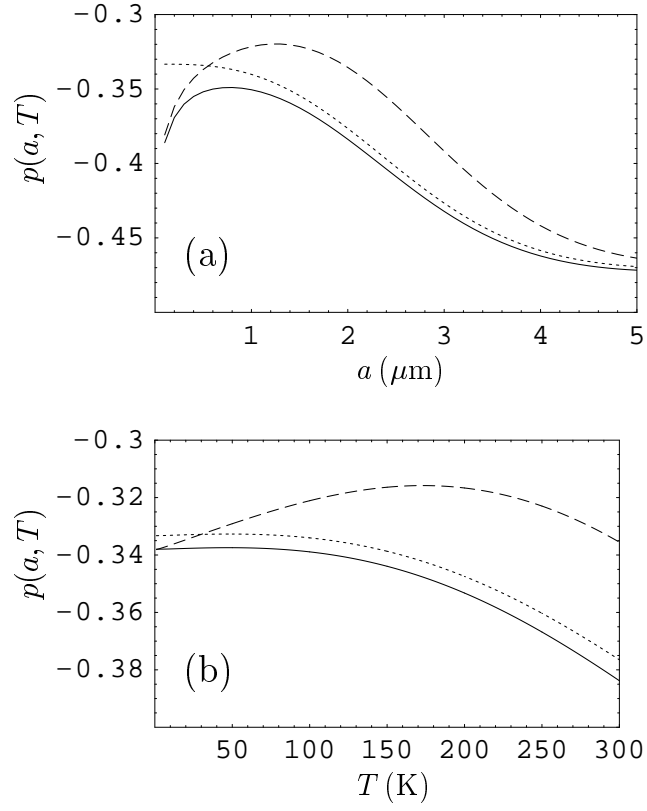


FIG. 3: The quantity p characterizing differences between the two formulations of the PFA for the gradient of the Casimir force as a function of (a) separation at room temperature $T = 300\text{ K}$ and (b) temperature at a separation $a = 2\ \mu\text{m}$. The dotted, dashed and solid lines show the results computed using ideal metals, Drude and plasma model approaches, respectively. The sphere radius $R = 100\ \mu\text{m}$.

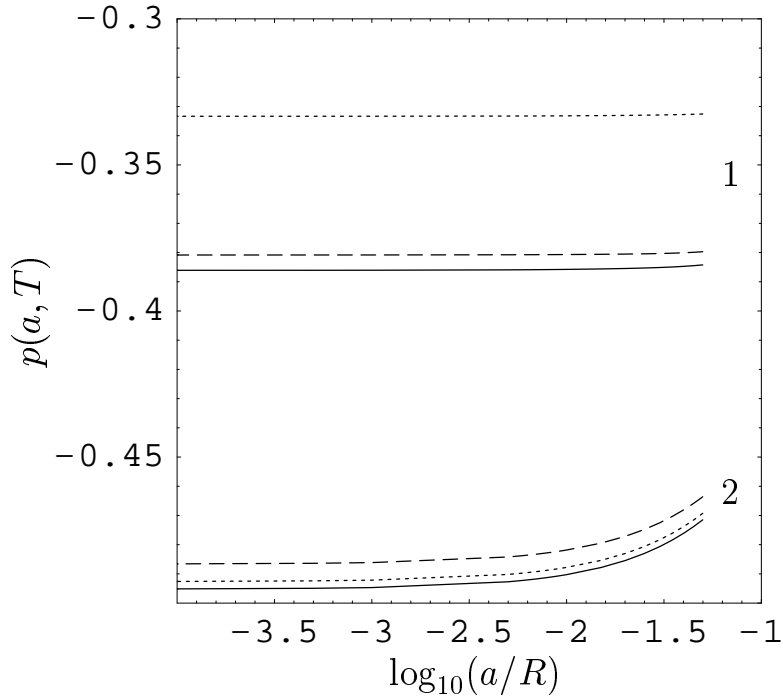


FIG. 4: The quantity p characterizing differences between the two formulations of the PFA for the gradient of the Casimir force as a function of a/R at room temperature $T = 300$ K. The dotted, dashed and solid lines show the results computed using ideal metals, Drude and plasma model approaches, respectively. The groups of lines numerated 1 and 2 are for the respective fixed separations $a = 0.1$ and $5 \mu\text{m}$.

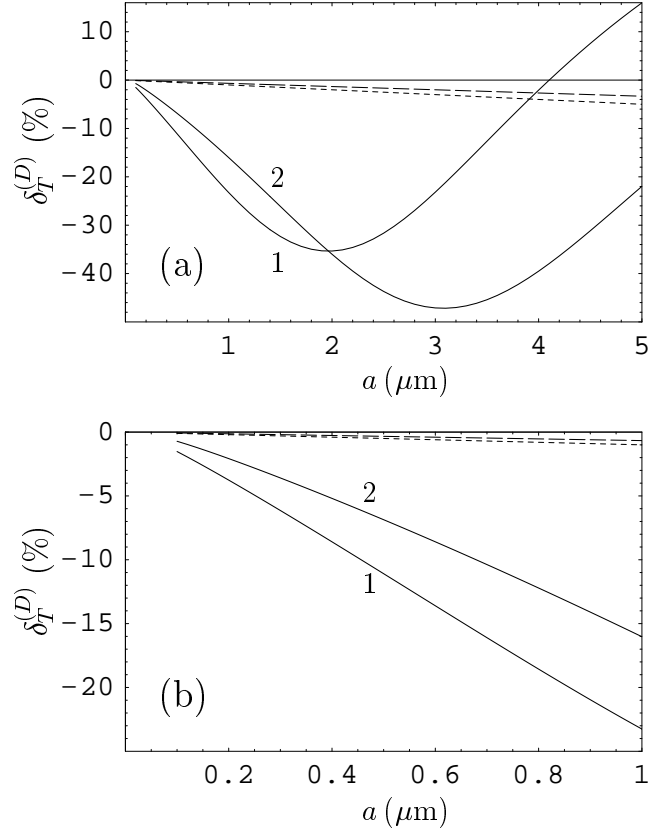


FIG. 5: Relative thermal correction to the Casimir force (the solid line 1) and to the Casimir pressure (the solid line 2) computed using the Drude model approach at $T = 300\text{K}$ over the separation region (a) from 0.1 to $5\mu\text{m}$ and (b) from 0.1 to $1\mu\text{m}$. The short-dashed and long-dashed lines show the quantity a/R for $R = 100$ and $150\mu\text{m}$, respectively.

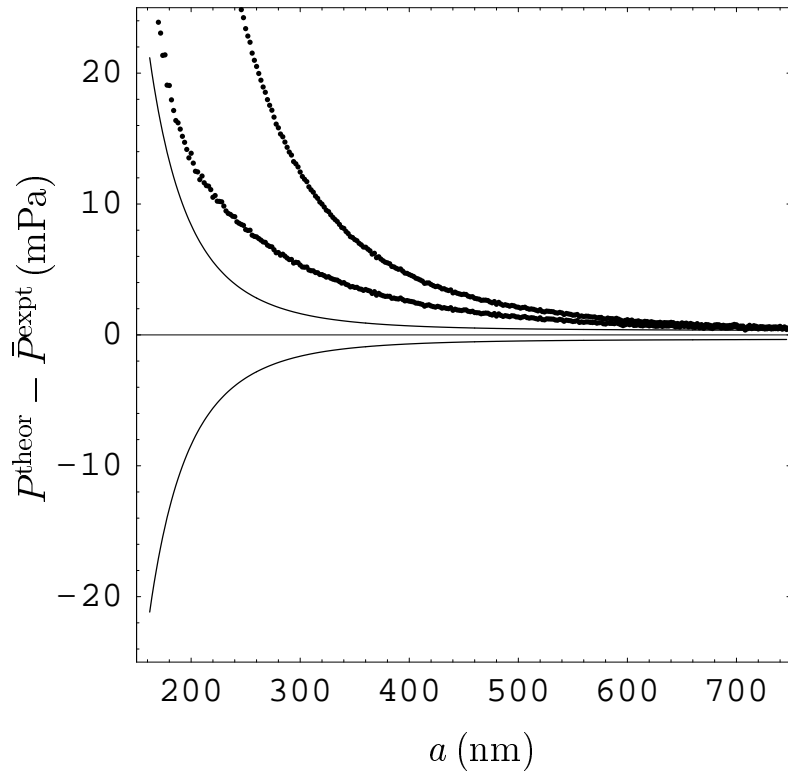


FIG. 6: Differences between the theoretical Casimir pressures, computed by means of the Drude model approach, and mean experimental Casimir pressures at different separations are shown as dots. The lower and upper sets of dots correspond to the use of conventional and alternative Drude parameters (see text for further details). The solid lines indicate the borders of the confidence intervals found at a 95% confidence level.

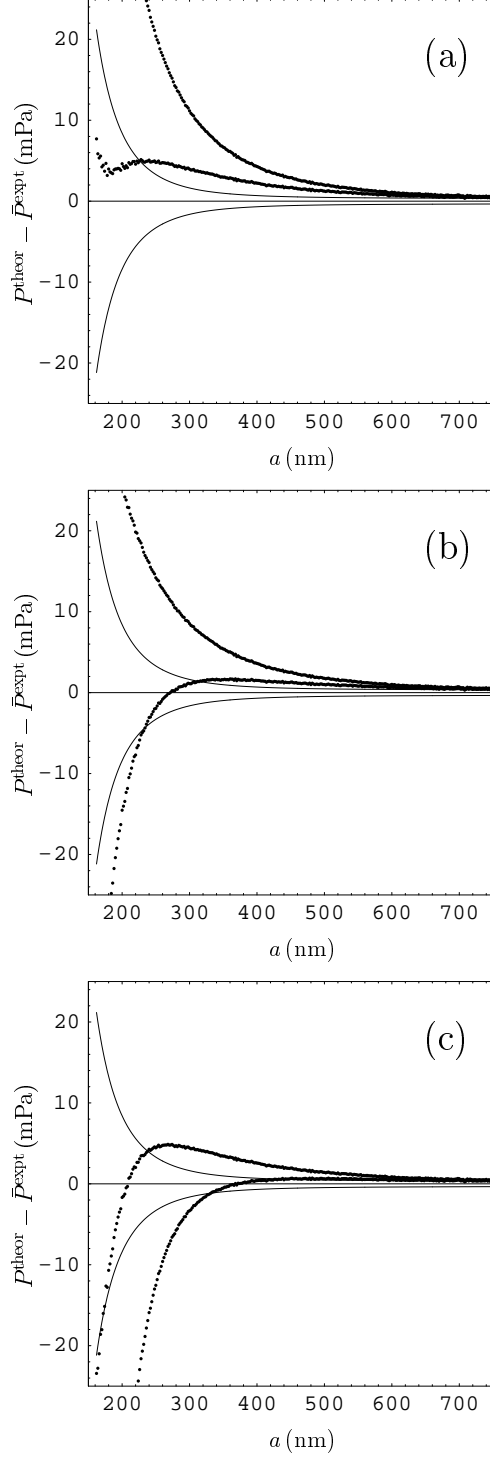


FIG. 7: Differences between the theoretical Casimir pressures, computed by means of the Drude model approach, and mean experimental Casimir pressures at different separations are shown as dots. Compared to Fig. 6, all separation distances are decreased by (a) $\Delta a = 1$ nm, (b) $\Delta a = 3$ nm and (c) $\Delta a = 6$ nm.

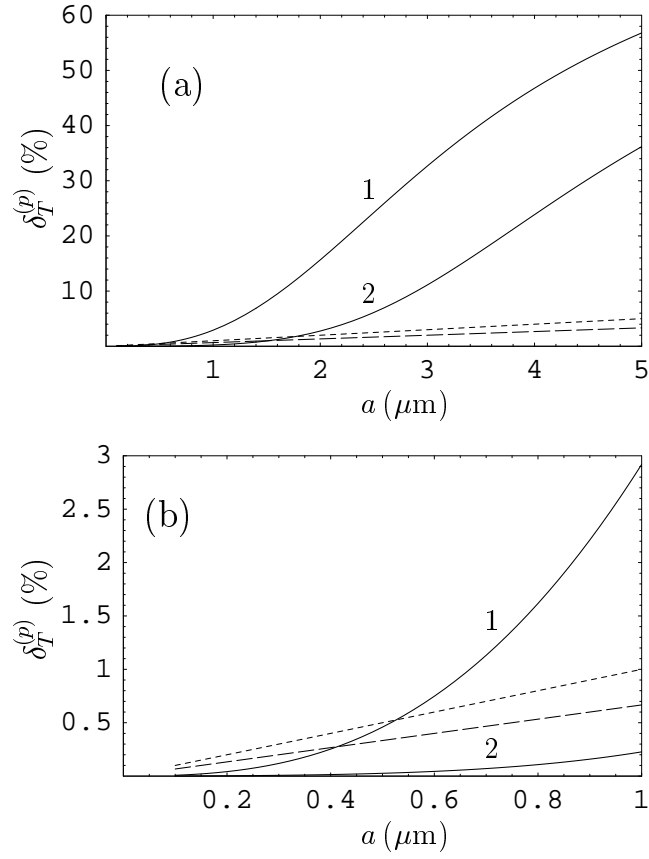


FIG. 8: Relative thermal correction to the Casimir force (the solid line 1) and to the Casimir pressure (the solid line 2) computed using the plasma model approach at $T = 300 \text{ K}$ over the separation region (a) from 0.1 to $5 \mu\text{m}$ and (b) from 0.1 to $1 \mu\text{m}$. The short-dashed and long-dashed lines show the quantity a/R for $R = 100$ and $150 \mu\text{m}$, respectively.

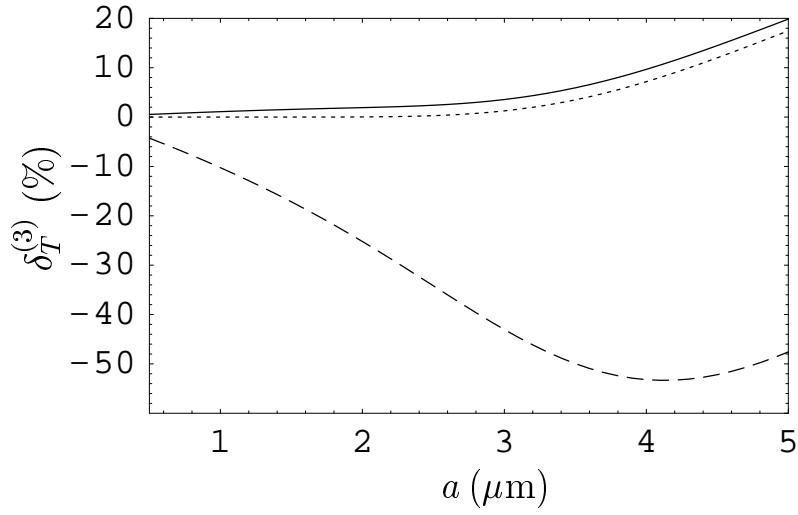


FIG. 9: Relative thermal correction to the gradient of the Casimir pressure between two parallel plates as a function of separation computed at $T = 300$ K using ideal metals (the dotted line), and the Drude and plasma model approaches (the dashed and solid lines, respectively).